Friction https://mc03.manuscriptcentral.com/friction
https://doi.org/10.26599/FRICT.2026.9441336

Review

Recent advances in lubrication mechanisms of electrospun nanofibers: Oil-mediated and non-oil strategies

Yuri Park [1], Geon Heo [2], Chan-Hyun Cho [1, 3], Si-Geun Choi [3], Myung Hyun Kim [3], Jaesang Yoo [3], Jongwan Choi [2], Myoung-Hwan Park [1, 2, ✉]

[1] Convergence Research Center, Nanobiomaterials Institute, Sahmyook University, Seoul 01795, Republic of Korea

[2] Department of Chemistry and Life Science, Sahmyook University, Seoul 01795, Republic of Korea

[3] High-Tech Bearing Technology Center, Korea Institute of Industrial Technology, Yeongju 36144, Republic of Korea

✉ Myoung-Hwan Park. E-mail: mpark@syu.ac.kr

Received: August 3, 2026; Revised: October 19, 2026; Accepted: November 10, 2026

© The Author(s) 2026.

Just Accepted

Abstract: Friction and wear develop inherently at the dynamic interfaces of moving devices, leading to considerable energy losses and shortened lifespans. To overcome these challenges beyond conventional methods, precise structural control of the contact interface is essential, and developing tailored lubricating structures is therefore imperative for modern machinery. By exploiting the high specific surface area, aspect ratio, and porosity, together with the interconnected three-dimensional network structure of electrospun nanofibers, this review discusses the effects of surface morphology

on lubricant behavior. Low-friction systems based on electrospun nanofibers are classified as oil-mediated self-lubricating nanofibers and non-oil interfacial and structural low-friction nanofibers. In oil-mediated systems, core-shell nanofibers store and release liquid lubricants from their internal cores, whereas non-core-shell nanofiber networks retain and structure oil to maintain an oil-rich lubricating environment. In addition, the friction reduction mechanisms are analyzed by focusing on lubricant storage and release, oil structuring, formation of hydration- and ion-based interfacial lubrication layers, reduction of interfacial shear resistance by solid lubricants, and the mechanical load-bearing effect of the nanofiber network. This review summarizes how nanofiber structure and material composition govern the friction and wear behavior of these systems.

Keywords: Electrospun nanofiber, Tribology, Oil reservoir, Coaxial nanofibers

Just Accepted

1 Introduction

Friction and wear are the primary factors that drive energy dissipation and component failure in mechanical systems. The literature indicates that friction accounts for approximately 30% of global primary energy consumption, whereas wear is implicated in approximately 80% of all component failures [1]. The resulting energy loss, coupled with performance degradation and escalating maintenance costs, imposes a substantial economic burden on the industrial sector. Accordingly, technologies that effectively reduce friction and control wear play an important role in improving the efficiency, reliability, and durability of mechanical systems [2-12].

Owing to their high specific surface area, aspect ratio, porosity, and interconnected three-dimensional network structure, electrospun nanofibers have attracted considerable attention as promising platforms for the development of low-friction and wear-resistant materials [13-16]. These structural features not only effectively store and retain lubricants or functional additives but also function as physical barriers that distribute contact loads and stresses over a wide area, thereby

preventing direct contact between opposing friction surfaces [17-23]. Furthermore, electrospinning offers a straightforward yet highly versatile route for processing diverse polymers and composites into nanofibrous matrices. This process allows meticulous control over critical fiber characteristics, including diameter, alignment, porosity, bead formation, and core–shell or multilayer configurations [18-23]. Consequently, electrospun nanofibers can be used as high-performance, low-friction, and wear-resistant architectural materials that extend beyond simple lubricant reservoirs. These structures perform multiple functions, including storing and supplying the lubricating medium, distributing loads, separating contact interfaces, and promoting the formation of hydration lubrication layers or protective tribofilms [24, 25].

The existing literatures on electrospinning have extensively covered the fundamental principles of the process, solution and operating parameters, material selection, architectural design, scale–up and application-specific functionalities [26-32,35-41]. Fibers with core–shell, hollow, aligned, porous and multilayer structures have also been extensively discussed, particularly regarding their manufacturing and applications in areas such as filtration, energy storage, sensing, wound healing and drug delivery [28-32,42-59]. However, these reviews are mainly organized according to manufacturing methods, material types and application areas, which limits the systematic comparison of how different electrospun systems reduce friction and wear in real sliding interfaces through distinct interfacial mechanisms.

Although recent studies on the tribological behavior of electrospun matrices and membranes have quantitatively evaluated friction, wear, load-bearing behavior and hydration effects [18-25,33,34], the relevant studies are still dispersed across various fields, including engineering lubrication, grease structuring, polymer wear and biomedical lubrication.

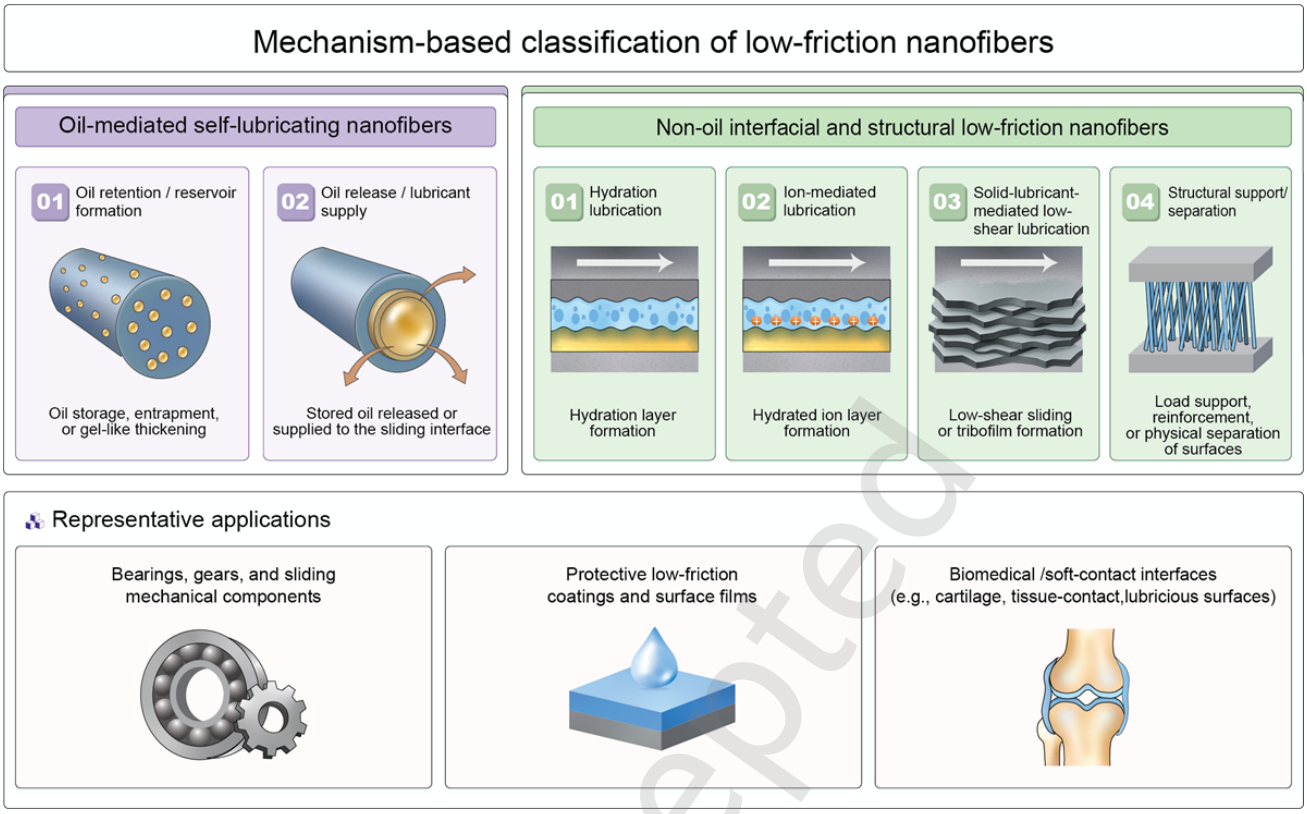
In addition, coefficients of friction (COF) reported in different studies are difficult to use as direct performance comparison metrics because counterpart materials, contact geometries, loads, sliding speeds and lubrication environments vary substantially. Furthermore, it remains difficult to

Just Accepted

quantitatively evaluate the relationships between nanofiber structural parameters and tribological performance, and the individual contributions of different lubrication mechanisms have not always been directly demonstrated under actual sliding conditions. Therefore, electrospun tribological systems should be compared based on the lubrication pathways operating at the contact interface and the corresponding test conditions, rather than solely on their constituent materials. This review classifies electrospun tribological systems into oil-mediated and non-oil systems according to their dominant lubrication mechanisms. The oil-mediated systems are distinguished into core-shell structures that store and release liquid lubricants from the fiber interior and non-core-shell structures in which nanofiber networks retain and structure the oil. The non-oil systems are further categorized into hydration lubrication, ion-mediated interfacial lubrication, solid or low-shear lubrication, mechanical reinforcement and load-bearing effects.

This review does not propose a universal quantitative correlation between fiber structure and COF, but systematically compares how nanofiber structures and components contribute to lubricant storage and delivery, interfacial layer formation, shear resistance reduction, load‑bearing capacity and wear resistance. In addition, direct experimental evidence and proposed mechanisms are discussed separately. This mechanism-based comparison identifies the common lubrication pathways across different electrospun systems and distinguishes the roles of nanofiber structures in friction and wear reduction. **Table. 1** shows representative tribological test conditions and friction and wear performance, while **Table. 2** summarizes the supporting evidence and limitations associated with the main lubrication mechanisms. **Scheme. 1** illustrates the overall organization of this review along with the mechanism-based classification framework.

Just Accepted



Scheme. 1 Schematic diagram illustrating the mechanism-based classification and representative application examples of low-friction electrospun nanofibers.

Just Accepted

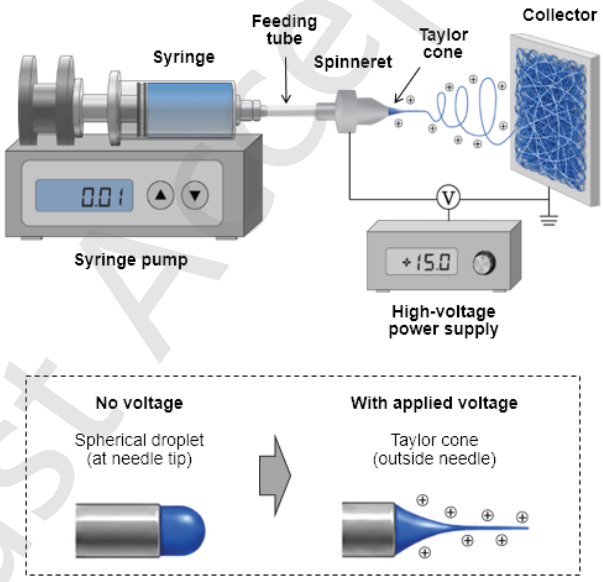
2 Electrospinning

2.1 Principle and Fabrication Methods of Electrospinning

Electrospinning is an electrohydrodynamic process that forms a charged liquid jet by applying a high voltage to a polymer solution or melt, thereby fabricating continuous fibers with micrometer- to nanometer-scale diameters within an electric field [35-37]. A typical electrospinning device comprises a high-voltage power supply, syringe, syringe pump, spinneret (typically a blunt-tipped metal needle), and a conductive collector that is either grounded or connected to an opposite potential [37-39]. As the applied voltage increases, electrostatic forces overcome the surface tension of the polymer droplet at the spinneret tip, causing the droplet to deform into a Taylor cone. Once a critical voltage is reached, a charged jet is ejected from the cone apex **(Scheme. 2)** [13, 36, 37]. During its travel toward the

collector, the jet undergoes stretching and bending instability accompanied by solvent evaporation and a progressive decrease in diameter, ultimately solidifying and depositing as micro or nanofibers.

The final structure of the fibers can vary considerably depending on the solution composition, nozzle design, fluid supply method, electric field, and collector type [40, 41]. Single-nozzle electrospinning can be used to fabricate not only uniform solid nanofibers, but also complex and phase-separated structures through blend or emulsion systems. Coaxial or multiaxial electrospinning can be used to fabricate nanofibers with well-defined internal structures, such as core–shell, multilayered, and hollow configurations. Accordingly, the following section discusses electrospinning strategies for controlling the nanofiber composition and internal structure, focusing on single-nozzle and coaxial/multiaxial electrospinning.



Scheme. 2 Schematic illustration of the electrospinning process, including Taylor cone formation and jet evolution.

2.2 Coaxial Electrospinning

Coaxial electrospinning is a method for fabricating core-shell-structured nanofibers by simultaneously supplying two different fluids through concentrically aligned inner and outer nozzles [42–45]. Typically, a coaxial nozzle comprises a small-diameter inner needle inserted into a large-diameter outer needle, where the core and shell fluids are supplied independently by separate syringe

Just Accepted

pumps [46–49]. When the two fluids meet at the nozzle exit, a compound Taylor cone forms under an external electric field. Subsequently, a coaxial jet is ejected with the shell fluid surrounding the core fluid, resulting in the formation of compositionally separated core–shell nanofibers. To form stable core–shell structures, the core and shell fluids must maintain a concentric compound jet during electrospinning [50, 51]. To achieve this, the flow rate ratio, viscosity, chain entanglement, surface tension, interfacial tension, electrical conductivity, permittivity, and miscibility of the two fluids must be appropriately controlled [52–54]. In particular, the flow rate ratio directly affects the core diameter, shell thickness, overall nanofiber diameter, and core continuity. If the two fluids mix rapidly, it is difficult to maintain a distinct interface between the core and shell [55, 56]. As such, fluid combinations with immiscible or limited miscibility characteristics are advantageous for forming stable core–shell structures [48-50].

In coaxial electrospinning, the shell fluid can serve not only as a simple shell material, but also as a supporting, protective, or sacrificial layer for stable jet ejection [46, 48]. These characteristics are highly useful for fabricating fibers from materials that are difficult to electrospin alone or that possess low morphological stability. Furthermore, they can be used to fabricate hollow or various hierarchical nanofiber structures via post-treatment [56-59]. However, if the physical properties or supply conditions of the two fluids are not properly controlled, defects such as core discontinuities, bead formation, fiber breakage, interfacial mixing, or structural collapse can occur. Consequently, in coaxial electrospinning, it is crucial to precisely control the rheological and electrical properties of fluids, as well as their interfacial behavior [51, 52, 54].

3. Electrospun Nanofibers

The tribological performance of electrospun nanofibers is determined by both their structural characteristics and material compositions. **Table. 1** provides an overview of representative systems, classifying their lubrication mechanisms according to nanofiber structure, functional components, and

Just Accepted

corresponding friction and wear performance. These structural and material factors are discussed

Polymer/system	Nanofiber structure	Functional component	Contact/counterface	Load/speed/duration	Environment	Control	COF result	Wear result	Ref.
Lignin/Ethylcellulose or lignin/PVP-based grease	Particle-like, bead-on-string, and bead-free structures	Castor oil	CSM ball-on-disc; 1 mm 115Cr V3 steel ball steel disc; pure sliding	Load: 0.4, 0.7, 0.9 N (1.60–2.10 GPa Hertzian) Sped/duration: 40 mm/s ; 20 min; ten repeated tests on track	Grease applied before test; 21 ± 1 °C	Different morphologies and neat castor oil	0.123 → 0.071 approximately 42.3% lower	Wear volume 430 → 70 μm³ approximately 83.7% lower	[3]
PVA/PAA/GO hydrogel reinforced with an electrospun membrane	Aligned multilayer membrane, four-layer reinforcement	Water-containing hydrogel interface	Not specified	Load: 40 N; Speed: 10 mm/s; durability: up to 500,000 friction cycles	Not specified	Unreinforced hydrogel	0.078 → 0.039 approximately 50% lower	Not quantitatively Reported	[18]
PA 6(3)T nanofiber mat	Fiber diameter: 463 ± 64 nm thermally formed inter-fiber junctions	No added lubricant	Modified ASTM D-3884-09 Taber abrasion; H-38 wheels	Load: 25 or 100 g Speed/duration: 240 mm/s; 10–1000 cycles	Dry	Untreated electrospun mat	0.86 → 0.49 at 100g load approximately 50% lower	2.14×10^{-5} → 3.66×10^{-6} g/cm at 100 g load Wear rate approximately 90% lower	[80]
PCL-g-poly(DMA-co-MPC) nanofibrous membrane	Zwitterionic polymer grafted onto PCL nanofibers	Hydration layer and bound water	UMT-5 rotation; 6 mm GCr 15 steel ball / membrane	Load: 0.5 N (also 0.5–3 N) Speed/duration: 50 mm/min (also 15–120 mm·min−1); radius 3 mm	DI water; air/water comparison	Pristine PCL membrane	0.32 → 0.10 approximately 65% lower	Not quantitatively Reported	[20]
PS/graphite-shell Silicone oil-core composite	Core–shell fibers containing 2 wt% graphite in the PS shell	Silicone oil and graphite	Pin-on-disk; steel pin / composite disk	Load: 15 N; Speed: 0.1 m/s	Self-lubricating; no external lubricant	Neat epoxy composite	0.32 → 0.08 approximately 75% lower	Wear rate 2.33×10^{-4} → 1.01×10^{-4} mm³/N·m approximately 56.7% lower	[84]
Ethylcellulose nanofiber in castor oil dispersion	Entangled ethylcellulose nanofibrous network	Castor oil	Ball-on-three-plates tribological cell; 1.4401 steel ball / 1.4301 steel plates	Load: 30 N Speed/duration: 50 rpm; 600 s	23 °C	Thermogel-based oleogel	0.110 → 0.075 approximately 31.8% lower	Wear-scar diameter 433.1 → 359.7 μm approximately 16.9% lower	[17]

separately in Sections 3.1 and 3.2.

Just Accepted

Table. 1 Representative tribological test conditions and performance of electrospun nanofiber-based systems.

3.1 Structural and Morphological Features of Electrospun Nanofibers

Electrospun nanofibers differ from conventional bulk- or film-type materials because of their unique fibrous architecture, including nanometer-scale fiber diameter, high specific surface area, high porosity, and interconnected fibrous network structures [15, 60]. These characteristics provide large interfacial areas, internal spaces for functional components, and opportunities for surface modification [14, 60]. Moreover, fiber diameter, surface chemistry, topology, porous structure, and internal structure can be controlled by adjusting electrospinning parameters, solution composition, collector design, and post-treatment conditions [13, 14, 61].

3.1.1 Porosity

A porous fibrous network is one of the representative structural characteristics of electrospun nanofibers. As porous nanofibers simultaneously offer high specific surface areas and internal spaces, they are highly advantageous for various functional applications requiring adsorption, storage, molecular loading, and mass transport [62, 63]. This interconnected porous structure serves as an effective pathway for storing or transporting liquids or functional components within a fiber network. In lubrication systems, these porous fibrous networks can also influence the oil storage, gradual release behavior, and stability of the contact interface [3].

3.1.2 Alignment

Fiber alignment is another important structural feature of electrospun nanofibers. Random mats form a nearly isotropic porous network, whereas aligned mats have a more regular spatial structure and directionality. Such aligned structures are important in the design of functional nanofibers because they enable direction-dependent control of the mechanical properties, charge or mass transport, deformation behavior, and interfacial responses [18, 39].

3.1.3 Core-Shell

Just Accepted

Coaxial or multiaxial electrospinning enables the fabrication of nanofibers with well-defined internal structures such as core–shell, hollow, and multilayered configurations [46, 54]. These core-shell structures enable the spatial separation of distinct components, offering distinct advantages for protecting internal materials or controlling their release into the external environment [54, 64]. Likewise, hollow or porous fibers can increase both the internal space and surface area, making them highly useful in systems requiring storage, adsorption, and release capabilities [46, 62].

3.1.4 Bead Formation and Surface Roughness

Bead formation and rough surface morphology in electrospun nanofibers have traditionally been considered morphological defects, as they hinder the fabrication of uniform fibers. However, in specific applications, such nonuniform structures can provide additional surface areas and serve as localized reservoirs for functional components [65]. Thus, the bead-on-string morphology and surface roughness are not merely defects to be eliminated; rather, they can serve as controllable structural features, depending on the application purpose [65].

Overall, these structural features can provide a foundation for low-friction and wear-resistant performance by enabling lubricant storage, controlled release, interfacial layer formation, load distribution, and separation of contact surfaces.

However, the individual contributions of these structural parameters to tribological performance have not been fully established. **Table. 2** summarizes their functional roles, reported tribological responses, experimental evidence, proposed mechanisms, and potential failure modes. The quantitative relationships between structural parameters and tribological performance are further discussed in Section 4.

Just Accepted

Structural parameter	Functional role	Quantitative tribological evidence	Experimentally demonstrated	Mechanistically inferred	Not directly verified	Design trade-off / failure mode	Ref.
Porosity / interconnected network	Oil retention & oil structuring & lubricant transport	COF 0.11–0.18 Wear diameter 440–860 μm	Composition- and morphology-dependent rheological and tribological properties	Network-mediated oil structuring and lubricant availability	Independent porosity effects and interfacial oil supply	Oil retention and mobility	[25]
Fiber diameter / morphology	Interfacial area & network formation	No isolated diameter–COF relationship reported	Changes in fiber morphology and oleodispersion properties	Morphology -dependent oil structuring	Independent diameter effects on COF and wear	Interfacial area and structural stability	[25]
Fiber alignment / ordered multilayer architecture	Directional reinforcement & Load support & Reduced liquid exudation	COF 0.045 (PPG-2) → 0.039 (PPG-4), 30 N, 5 mm/s Tensile strength 13.7 ± 1.5 MPa (PPG-4)	Layer-dependent mechanical and tribological improvements	Improved load distribution and reduced liquid exudation	Independent effect of fiber alignment	Reinforcement and flexibility	[18]
Core–shell architecture	Internal lubricant storage and release	COF reduction: ~70% Wear rate reduction: ~50% vs neat epoxy	Core–shell fabrication & Reduced COF and wear	Oil release and graphite-mediated lubrication	Individual lubricant contributions and release kinetics	Potential premature sh ell failure and lubricant depletion	[82]
Bead formation / surface roughness	Local reservoirs & surface contact modification	No direct tribological data in cited source	Formation and morphological control of bead-on-string fibers	Potential local lubricant retention	Bead-dependent COF and wear	Stress concentration and bead detachment	[65]
Interfiber junctions / structural integrity	Mechanical reinforcement & Load support	COF reduction: ~50% Wear rate reduction: ~90% After thermal annealing	Mechanical properties: 2–10-fold improvement COF reduction: ~50% Wear rate reduction: ~90%	Enhanced load support and reduced fiber damage	Independent contribution of junction density	Reduced porosity and observed fiber debris	[80]
Network densification / MWCNT reinforcement	Network strengthening & Wear resistance	Minimum COF 0.15 Abrasive mass loss 0.2 mg (5 wt% MWCNT, hot-pressed)	Increased tensile strength Reduced friction and abrasive mass loss	Mechanical reinforcement and possible graphitic lubrication	Separate effects of MWCNTs, densification and graphitic phases	Potential structural damage under repeated sliding	[95]

Table. 2 Relationships between structural parameters, functional roles, tribological responses, potential failure modes, and limitations of the available evidence in electrospun nanofibers.

3.2 Materials for Low-Friction Electrospun Nanofibers

3.2.1 Polymers

Polymer materials suitable for electrospinning can serve either as functional surface materials or as structural matrices in low-friction systems. Fluorinated polymers such as poly(vinylidene fluoride) (PVDF) and poly(vinylidene fluoride-co-hexafluoropropylene) possess low surface energy and tunable wettability [66-69]. Polyimide-based nanofibers provide high thermal stability, mechanical strength, and toughness and can serve as mechanically stable porous matrices [70-77]. Other common electrospinnable polymers, including polycaprolactone (PCL), poly(lactic acid) (PLA), polyamide (PA), and poly(vinyl alcohol) mainly function as structural matrices that support the nanofiber network and immobilize functional lubricating components [78-80]. In core–shell systems, polymer shells can additionally protect internal components and control their release [54].

3.2.2 Liquid Lubricants

Various liquid lubricants including silicone oils, bio-based oils, synthetic oils, ionic liquids, and functional liquid lubricants can be stored in electrospun nanofiber networks or core-shell structures and subsequently released during sliding contact [81, 82]. In this system, the nanofibers act not only as solid supporting matrices but also as reservoirs and release control layers for lubricant components [82, 83].

Just Accepted

3.2.3 Solid Lubricants and Fillers

Solid lubricants or carbonaceous fillers relevant to electrospun tribological systems include graphite, carbon nanotubes (CNTs), graphitic carbon, and layered solid lubricants such as MoS_2 [84-87]. In particular, in core–shell electrospun fibers, an oil-containing core and a graphite-containing shell can provide a dual lubrication mechanism in which liquid and solid lubricants act simultaneously [82].

3.2.4 Hydrophilic/Zwitterionic Components

Hydrophilic or zwitterionic components can strongly interact with water molecules and are therefore useful for designing water-mediated low-friction interfaces [88]. Zwitterionic materials such as poly(2-methacryloyloxyethyl phosphorylcholine) PMPC and lecithin have been incorporated into electrospun nanofibers for biolubricating and anti-adhesive applications [89].

Ultimately, the design of electrospun nanofibers for low-friction applications should not be interpreted merely in terms of the intrinsic lubricity of a specific material. Rather, the actual low-friction performance arises from the combined effects of the polymer-based structural support, storage, and release of liquid lubricants, interfacial protection by solid lubricants, and hydration lubrication by hydrophilic or zwitterionic components. These material-specific functions are further discussed in Section 4 in terms of the oil-mediated self-lubrication and non-oil interfacial and structural lubrication mechanisms.

Just Accepted

4. Lubrication Mechanisms of Electrospun Nanofibers

4.1 Oil-mediated Self-Lubricating Nanofibers

Oil-mediated self-lubrication is one of the most direct strategies for achieving low friction and wear-resistance using electrospun nanofibers. In this approach, the electrospun nanofibers contribute to the storage, retention, and supply of liquid lubricants through different structural mechanisms. In core-shell systems, liquid lubricants are stored within the fiber core and released to the friction surface when the shell is damaged during sliding contact. In contrast, non-core-shell systems retain and structure oil

within interconnected nanofiber networks, maintaining an oil-rich lubricating environment without requiring lubricant release from an internal fiber core. In both systems, the liquid lubricant can mitigate direct contact between the counter surfaces, reduce interfacial shear resistance, and inhibit the progression of wear. Therefore, although both systems rely on liquid lubrication, the structural roles of electrospun nanofibers differ in lubricant storage, release, and oil structuring.

4.1.1 Core-Shell Oil-Mediated Self-Lubricating Nanofibers

Arashpour et al. fabricated a self-lubricating epoxy/carbon fabric composite using a coaxial electrospinning process and demonstrated simultaneous improvements in both mechanical and tribological properties [82]. In this study, core–shell electrospun fibers were fabricated using silicone oil as the core and polystyrene containing 2 wt% graphite nanoparticles as the shell (**Fig. 1(a)** and (**b)**). The fabricated core-shell fibers were deposited onto carbon fabric layers and subsequently impregnated with an epoxy matrix, which served as a self-lubricating component within the composites. The authors attributed the low-friction performance of these systems to a dual-lubrication mechanism in which liquid and solid lubricants acted simultaneously. When the polystyrene shell was damaged and worn during sliding contact, the silicone oil stored in the core was released, forming a liquid lubricating layer at the friction interface. Simultaneously, the graphite nanoparticles contained in the shell were considered to serve as solid lubricants with low shear resistance, suppressing direct contact and wear at the sliding interface.

To evaluate the tribological performance of the fabricated self-lubricating composite, a pin-on-disk wear test was conducted under steel pin-on-composite disk contact conditions. The composites showed reductions in the COF and wear rate of approximately 70% and 50%, respectively, compared with pure epoxy (**Fig. 1(**c) and (**d)**). The authors attributed these improvements to the combined contributions of silicone-oil release and graphite-mediated solid lubrication. However, the individual contributions of silicone-oil release and graphite-mediated lubrication were not independently quantified. These results

Just Accepted

indicate that core–shell electrospun fibers can act as reservoirs for liquid lubricant storage and release, while the solid lubricant components in the shell can complement oil-mediated self-lubrication.

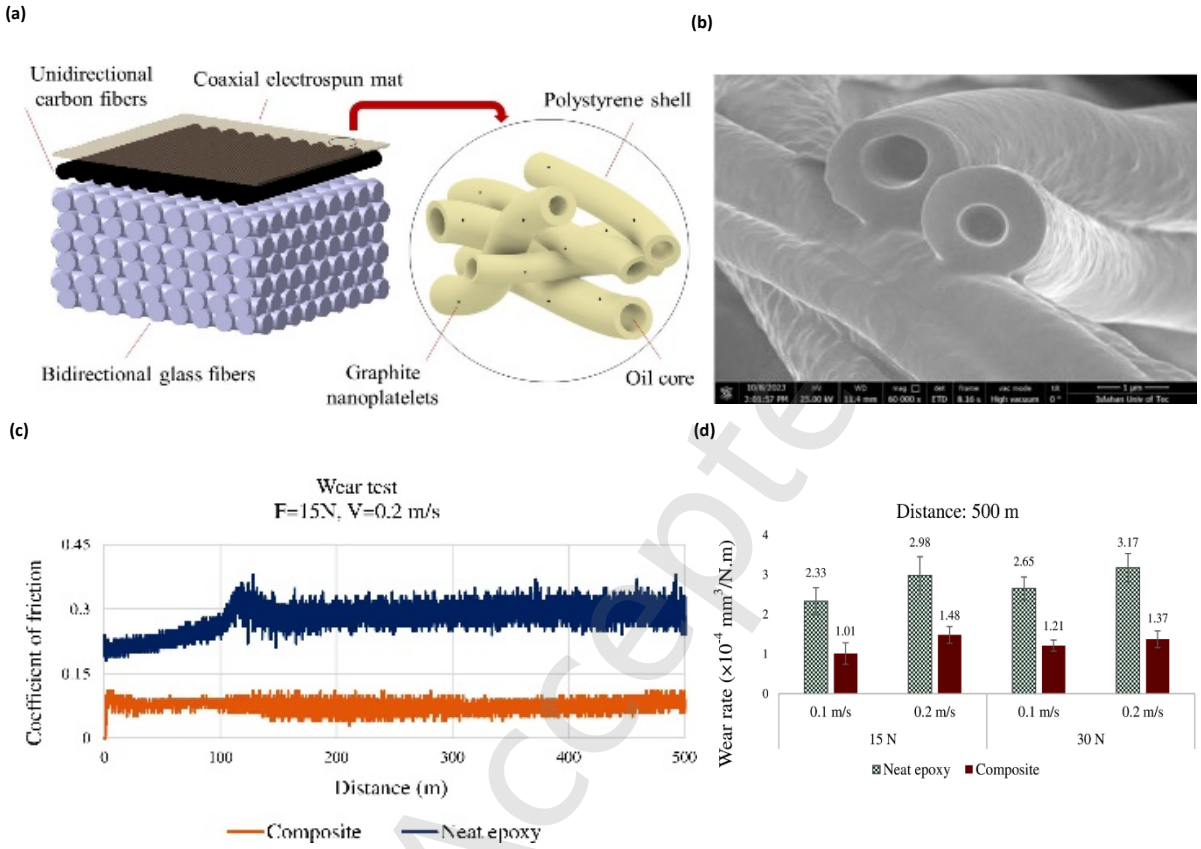


Fig. 1(a) Schematic representation of the arrangement of fiber layers in the composite, (b) cross-sectional FE-SEM image of the electrospun core–shell fibers, (c) friction coefficient, and (d) wear rate of the composites.

4.1.2 Non-Core–Shell Oil-Mediated Self-Lubricating Nanofibers

Borrego, Franco, Martín-Alfonso, and co-workers reported a series of studies using electrospun nanofibers as structuring agents for castor oil [90, 91]. In these studies, bio-based oleogels or grease-like lubricants were developed by dispersing various electrospun nanofiber structures, including lignin/PVP [91], lignin/ethylcellulose [21], ethylcellulose [17], cellulose acetate butyrate [22], cellulose acetate propionate [90], and lignin/PCL [25], in castor oil.

As a representative example, studies on cellulose acetate propionate illustrated the manufacturing process of electrospun nanofiber structures and the formation of oleodispersions in castor oil (**Fig. 2(a)**) [90]. Although these systems do not store oil inside the fibers in a core–shell structure, electrospun

Just Accepted

nanofibers form entangled three-dimensional physical networks within the oil. These networks are considered to entrap and immobilize the oil, thereby reducing its flowability, and consequently impart a gel-like rheological behavior. In an early study, Borrego et al. fabricated oleogel-based lubricant systems by dispersing 10–30 wt% lignin/PVP electrospun nanofiber mats in castor oil.

In these systems, the nanofiber network acts as a thickener that physically structures and stabilizes liquid oil. The resulting oleogels demonstrated their potential as lubricants in friction and wear tests using a tribological cell [91]. Subsequent studies using electrospun nanofiber structures based on lignin/ethylcellulose, cellulose acetate, and lignin/PCL demonstrated that the polymer composition, fiber morphology, thickener concentration, and electrospinning conditions can control the rheological properties and tribological performance of these oleodispersions [21, 25].

In particular, studies based on lignin/ethylcellulose and cellulose acetate propionate have shown that the oil retention capacity, adhesiveness, storage modulus, friction, and wear behavior under metal-to-metal contact vary depending on the morphology and concentration of nanofibers. Some formulations exhibited lubricating performance comparable to that of conventional lithium-based greases (**Fig. 2(b)** and (**c)**) [90]. In addition, studies based on lignin/PCL have demonstrated that the fiber diameter and uniformity can be regulated by controlling the electrospinning parameters such as the applied voltage, flow rate, humidity, tip-to-collector distance, and collector type. As a result, the rheological and tribological properties of oleodispersions can be tailored [25].

Accordingly, these studies show that although electrospun nanofibers do not store liquid lubricants in an internal core, they can form non-core–shell oil-mediated lubrication systems by acting as thickener-like physical networks that entrap and structure the oil. However, these mechanisms should be understood as lubricating mechanisms based on oil structuring, oil retention, and maintenance of a stable oil-rich interface, rather than the direct release of oil.

Just Accepted

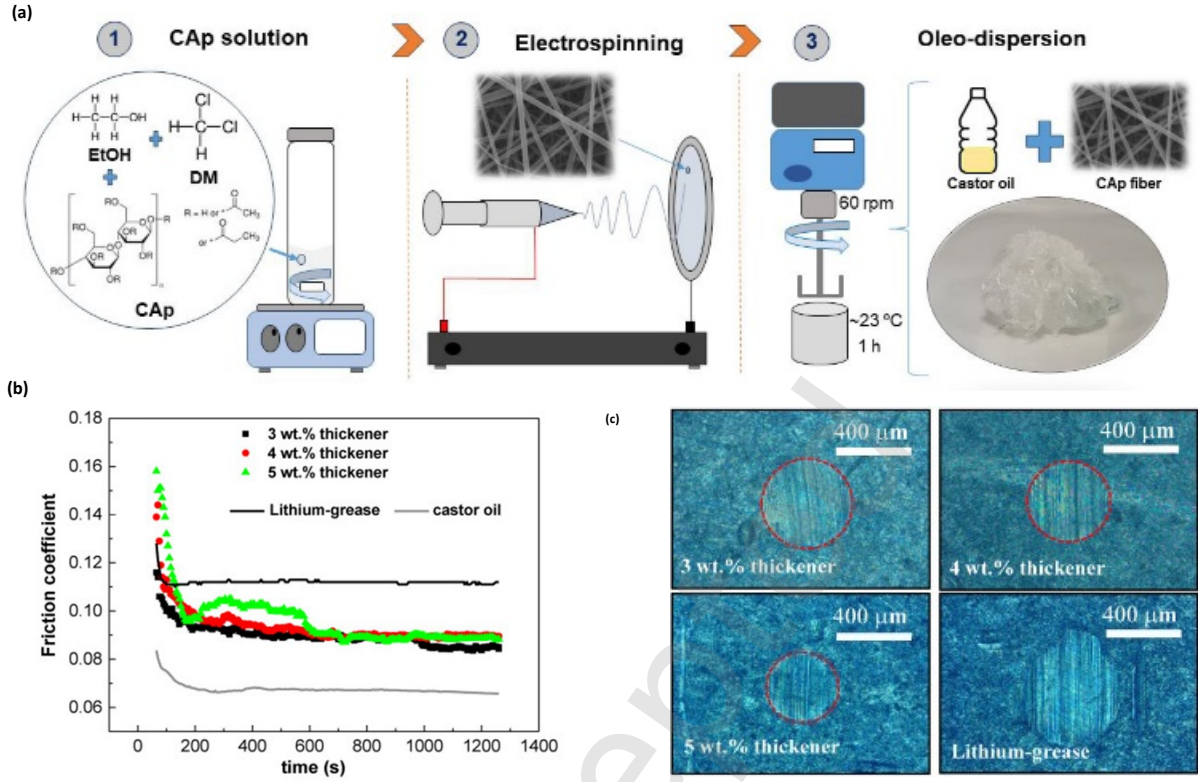


Fig. 2(a) Schematic flow diagram of the manufacturing process of cellulose acetate propionate oleodispersions. (b) Friction curves for oleodispersions as a function of thickener concentration. (c) Optical images of the worn plate surface for steel–steel contacts.

Unlike core-shell systems, where the fiber structure primarily governs the encapsulation and release of the lubricant, non-core-shell oleodispersions control oil retention and the formation of rheological structures through an interconnected fiber network. Therefore, although both systems ultimately rely on liquid lubricants to reduce friction, the tribological roles played by their respective nanofiber structures differ.

These structural differences may also influence lubricant supply and friction stability during prolonged sliding. In core–shell systems, lubricant availability depends on oil storage and release from the fiber core, whereas non-core-shell systems rely on oil retention and the stability of the nanofiber network. However, the relationship between these lubricant supply mechanisms and long-term tribological performance has not been systematically established. Further studies are needed to evaluate lubricant release and retention during sliding and their effects on long-term friction and wear performance.

Just Accepted

4.2 Non-oil Interfacial and Structural Low-Friction Nanofibers.

Non-oil interfacial or structural low-friction nanofiber systems represent a strategy for reducing friction and wear through the intrinsic nanofiber surface properties, solid lubricant components, interfacial layer formation, and structural support effects, rather than relying on the storage and release of liquid lubricants. Using this approach, the electrospun nanofibers can contribute to the formation of protective layers at the sliding interface and serve as matrices for the immobilization of solid lubricating fillers. Moreover, these systems can contribute to load distribution and structural stability between the contacting surfaces through their porosity, alignment, and fiber network structures. In particular, electrospun systems incorporating solid lubricating components such as graphite and MoS_2 can contribute to reducing interfacial friction through low shear resistance or interfacial layer formation. In addition, nanofibers containing hydrophilic or zwitterionic components can provide a water-mediated, low-friction interface by forming hydration layers. The mechanical stability, fiber alignment, and network structures of the electrospun nanofibers can also suppress structural collapse and wear debris generation during sliding contact, contributing to the mitigation of direct damage between the contacting surfaces. Accordingly, non-oil-based low-friction electrospun nanofibers can operate through distinct interfacial and structural mechanisms. In the following subsections, these mechanisms are separately discussed as hydration lubrication, ion-mediated interfacial lubrication, solid-lubricant-mediated low-shear lubrication, and mechanical reinforcement and load-bearing effects.

4.2.1 Hydration Lubrication

The ultralow–friction behavior of the articular cartilage is mainly associated with hydration lubrication. Phosphatidylcholine-based lipids present on articular surfaces possess zwitterionic structures and form stable hydration layers through the strong interactions between their zwitterionic head groups and water molecules. Strongly bound hydration layers can remain under high–load

Just Accepted

conditions and provide a slippery interface with low shear resistance, thereby suppressing direct contact between opposing surfaces [88, 89].

Inspired by the hydration lubrication mechanism of articular cartilage, Cheng et al. fabricated nanofiber membranes with enhanced hydration lubricity by the one-step *in situ* grafting of a copolymer composed of dopamine methacrylamide and 2-methacryloyloxyethyl phosphorylcholine (MPC) onto the surfaces of electrospun polycaprolactone (PCL) nanofibers [20]. MPC possesses zwitterionic structures that strongly bind water molecules to the nanofiber surfaces, forming a stable hydration layer and imparting hydration-lubricating behavior. Consistent with this mechanism, the fabricated lubricating nanofiber membrane exhibited a COF reduction of approximately 65% compared with pure PCL nanofibers. It also exhibited excellent wear resistance under sliding conditions (**Fig. 3**). By contrast, the pure PCL nanofibers tended to be easily worn during sliding contact, regardless of the hydration state.

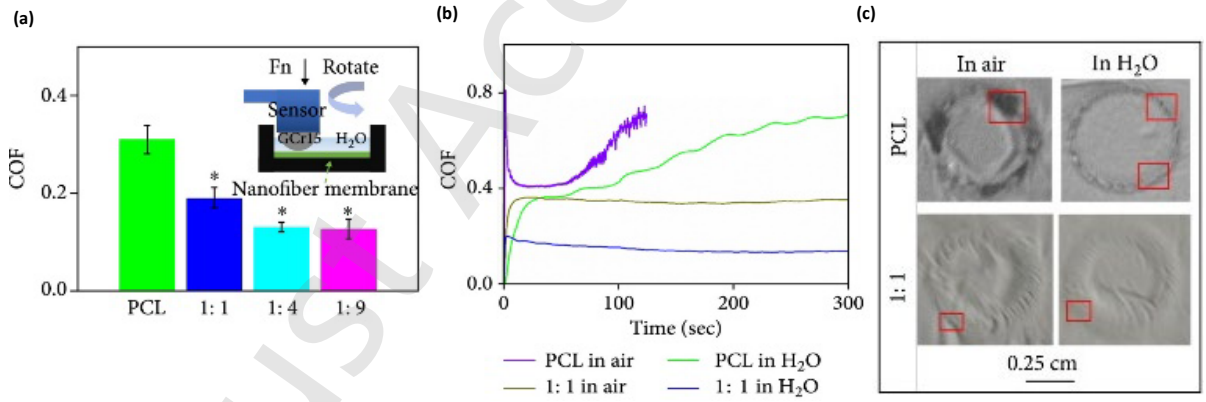


Fig. 3 Lubrication performance of the nanofibrous membranes. (a) Average COF values of the different samples. (b) Time-dependent COF curves of the PCL and 1:1 membrane under air and water conditions. (c) SEM images of the wear tracks on the PCL and 1:1 membrane after friction tests in air and water.

Inspired by the low–frictionsurface properties arising from an ultrathin and continuous bound water layer on an ice surface, Wang et al. fabricated PCL/PMPC composite nanofiber membranes via electrospinning under controlled relative humidity conditions. The zwitterionic PMPC introduced into the nanofibers formed bound-water layers on the surface and generated a hydration-lubricating surface

Just Accepted

(**Fig. 4(a)**) [92]. PCL/PMPC nanofibers fabricated under 20% relative humidity exhibited a minimum COF of approximately 0.12 at a PMPC/PCL weight ratio of 0.1. Under higher relative humidity conditions, ultra–lowfrictoinsurfaces with ultralow COF below 0.05 were formed on the composite nanofiber surfaces (**Fig. 4(b)** and (**c)**).

In a follow-up study, Wang et al. proposed an in situ growth strategy for forming superlubricated nanoskin (SLNS), as termed by the authors, on individual electrospun nanofiber surfaces [33]. The authors first electrospun PLA-based nanofibers, and subsequently induced the polymerization of MPC monomers using a photoinitiator contained within the nanofibers. During this process, zwitterionic PMPC polymer chains were formed through an inside-out growth mechanism, ultimately forming a robust network structure that interpenetrated the polymer chains of the nanofibers. The PMPC-based SLNS provided a stable bound-water layer on the surface, which reinforced its hydration-lubricating behavior. The SLNS-modified nanofiber membrane, referred to by the authors as the superlubricated nanofiber membrane (SLNM), exhibited a COF below 0.025 under sliding conditions using deionized water as the lubricating medium, which was approximately 16 times lower than that of the pristine nanofibers. The COF remained stable after 12,000 sliding cycles (**Fig. 4(d)** and (**e)**).

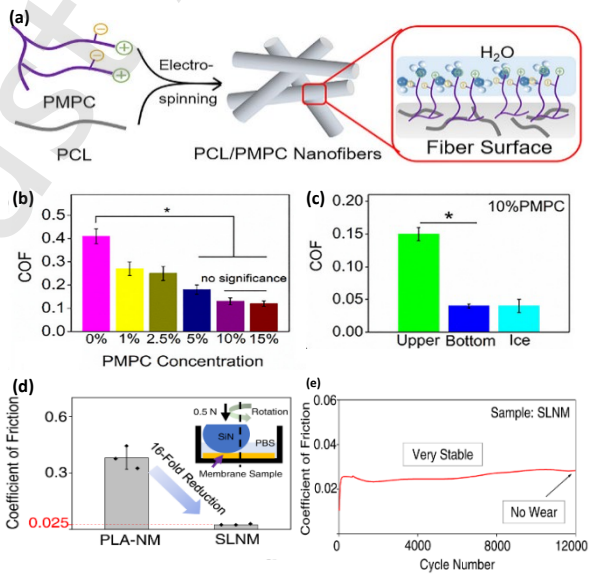


Fig. 4 (a) Illustration of the unique structure of the composite nanofibers. (b) Effect of PMPC content on the measured COF of the test samples. (c) COF of the top and bottom surfaces of samples fabricated

at 65% relative humidity compared with an ice surface. (d) Comparison of COF values between the PLA nanofibrous membrane (PLA-NM) and the superlubricated nanofiber membrane (SLNM) under rotational sliding conditions. (e) COF curve of the SLNM over repeated testing cycles.

Li et al. proposed a hydration lubrication-based strategy for preventing abdominal adhesion by developing electrospun lecithin/PLA nanofiber membranes (L/P-NMs) [24]. The zwitterionic properties of lecithin enable the formation of bound-water-based hydration layers on the nanofiber surfaces through strong interactions with water molecules. As the lecithin content increased, both the bound water content and lubricity improved. In particular, 20% L/P-NM exhibited a minimum COF of approximately 0.112 and demonstrated its potential as an anti-adhesion membrane by inhibiting fibroblast adhesion and reducing the adhesion scores in a rat abdominal adhesion model.

Collectively, these studies suggest hydration lubrication as a possible explanation for friction reduction in zwitterionic electrospun nanofiber systems. Although different zwitterionic materials and fabrication strategies were employed, including MPC surface grafting, PMPC incorporation, and lecithin addition, the reported low-friction behavior was commonly attributed to the interaction between zwitterionic groups and water molecules, which may promote the formation of hydrated interfacial layers with low shear resistance. However, the experimental evidence for these hydration layers remains mainly indirect. FTIR, XPS, EDS, and SEM were used to characterize the chemical composition and morphology of the nanofibers, while water contact angle and TGA/DTG measurements provided information on surface wettability and water-related thermal behavior. These results, together with the tribological performance, support the proposed hydration lubrication mechanisms but do not directly verify the formation or stability of hydration layers during sliding. **Table. 3** summarizes the proposed hydration mechanisms, characterization methods, experimental evidence, and limitations of these studies. In addition, the absolute COF values should not be directly compared among the studies because the counterface materials, loads, sliding conditions, and aqueous environments differed substantially.the interaction between zwitterionic groups and water molecules, which may promote the formation of hydrated interfacial layers with low shear resistance. However,

Just Accepted

the experimental evidence for these hydration layers remains mainly indirect. FTIR, XPS, EDS, and SEM were used to characterize the chemical composition and morphology of the nanofibers, while water contact angle and TGA/DTG measurements provided information on surface wettability and water-related thermal behavior. These results, together with the tribological performance, support the proposed hydration lubrication mechanisms but do not directly verify the formation or stability of hydration layers during sliding. **Table. 3** summarizes the proposed hydration mechanisms, characterization methods, experimental evidence, and limitations of these studies. In addition, the absolute COF values should not be directly compared among the studies because the counterface materials, loads, sliding conditions, and aqueous environments differed substantially.

Just Accepted

Nanofiber system	Hydration mechanism	Characterization methods and scope	Direct evidence of hydration layer	Indirect evidence	Evidence limitation	Ref.
MPC-grafted PCL	Zwitterionic MPC groups hydration through ion–dipole interactions	FTIR: MPC-related functional groups and polymer composition XPS: Surface elemental composition and phosphorus signals from MPC SEM: Fiber morphology and post-sliding wear damage WCA: Surface wettability Friction tests: COF and wear behavior in air and water	Not directly observed	MPC grafting water-dependent friction COF reduction of ~65%	Hydration layer formation and stability during sliding not verified	[20]
PCL/PMPC composite	Zwitterionic PMPC groups hydration through ion–dipole interactions	SEM: Fiber morphology, pore structure, and surface flattening EDS: Phosphorus distribution indicating PMPC enrichment WCA: Surface wettability TGA/DTG: Bound-water-associated thermal mass loss Friction tests: COF, wear damage, and friction stability	Not directly observed	PMPC surface enrichment bound-water signals COF below 0.05	Hydration layer continuity and stability during sliding not verified	[92]
PMPC nanoskin on PLA	Surface-grafted PMPC hydration through ion–dipole interactions	SEM: Nanoskin formation and preservation of fiber morphology XPS: Surface phosphorus signals confirming PMPC incorporation WCA: Surface wettability TGA: Thermal mass loss for composition-related analysis Friction tests: COF and sliding durability	Not directly observed	PMPC nanoskin formation COF below 0.025 stable for 12,000 cycles	Hydration layer persistence during repeated sliding not verified	[33]
Lecithin-containing PLA	Zwitterionic lecithin head groups hydration through ion–dipole interactions	SEM: Fiber morphology and diameter distribution WCA: Lecithin-dependent surface wettability TGA: Bound-water-associated thermal behavior Friction tests: COF in simulated body fluid Tensile tests: Tensile strength and deformation behavior	Not directly observed	Increased bound-water-related content minimum COF of ~0.112	Hydration layer formation and stability during sliding not verified	[24]

Table. 3 Experimental evidence and limitations of hydration lubrication in electrospun nanofibers.

Just Accepted

4.2.2 Ion-Mediated Interfacial Lubrication

Zheng et al. fabricated PVDF/CNT nanofiber membranes by incorporating CNTs into PVDF via electrospinning [93]. The incorporated CNTs influenced the alignment of PVDF chains and crystallization behavior, leading to the modulation of the ratio of α- and β-phases and simultaneous improvements in tribological and piezoelectric properties. Moreover, the CNTs improved the wettability and surface-potential stability by modifying the surface morphology, surface energy, and charge distribution of the nanofiber membrane. Consequently, simulated body fluid was more uniformly spread over the membrane surface, leading to the formation of an interfacial environment that facilitated the approach and stable adsorption of Ca^{2+} ions on the surface. The authors attributed the improved lubrication behavior partly to the adsorbed Ca^{2+} and associated hydrated ion layers, which were proposed to provide a biolubricating interface with reduced shear resistance. Thus, the PVDF/CNT membrane exhibited a lower COF than the pure PVDF membrane and retained its Ca adsorption capacity after the sliding tests. Accordingly, this study demonstrates that CNT incorporation improves the tribological performance of PVDF nanofiber coatings, accompanied by changes in surface wettability, surface potential, Ca^{2+} adsorption, and nanofiber structure. However, the individual contributions of ion adsorption, hydration effects, surface charge, and structural changes remain unresolved.

In this study, the contributions of ion adsorption, hydration effects, surface charge, and structural changes should be distinguished. XPS and EDS analyses provided information on surface chemical composition and Ca accumulation after immersion in simulated body fluid, but did not by themselves establish the adsorption state or hydration environment of Ca^{2+}. Surface potential measurements and structural analyses showed changes in surface electrical properties, nanofiber morphology, and PVDF crystalline phases [93]. These results support ion-related surface interactions and structural changes, but do not directly confirm the formation of hydrated Ca^{2+} layers during sliding. In addition, the individual contribution of Ca^{2+}-associated hydration to friction reduction was not independently

Just Accepted

determined. The improved wettability, changes in surface potential and crystalline phases, and modification of nanofiber morphology may also contribute to the observed friction reduction. Therefore, further studies using surface chemical analysis, zeta potential measurements, and controlled tribological tests with different ion species and concentrations are needed to distinguish these effects. In particular, comparisons under the same sliding conditions, together with direct characterization of interfacial hydration, would help clarify the contribution of ion-mediated hydration to friction reduction. Unlike zwitterionic hydration lubrication, this mechanism is associated with the adsorption and hydration of interfacial ions rather than the formation of bound-water layers directly around zwitterionic groups. Therefore, ion-mediated lubrication is considered separately from hydration lubrication in this review.

4.2.3 Solid-Lubricant-Mediated Low-Shear Lubrication

Solid lubricants reduce friction primarily by providing low-shear sliding interfaces without relying on liquid lubricant release. Layered solid lubricants such as graphite and MoS_2 can reduce interfacial shear resistance, and their rearrangement or transfer to the sliding interface can contribute to the formation of low-friction interfacial layers [84-87].

Recently, Liu et al. introduced MoS_2 nanosheets as a solid lubricant into an electrospun all-fiber sliding system to improve its friction and wear durability. The incorporation of MoS_2 reduced the kinetic friction coefficient by approximately 41.4% and enabled stable operation for up to 44,000 sliding cycles. The authors attributed this improvement to MoS_2 -mediated solid lubrication, in which the layered structure of MoS_2 reduces interfacial shear resistance during sliding [94].

Solid-lubricant contributions have also been reported as secondary mechanisms in other electrospun tribological systems. In the core-shell system discussed in Section 4.1.1, graphite nanoparticles in the shell were proposed to provide solid lubrication together with silicone-oil release [82]. In addition, graphitic structures formed during carbonization of MWCNT/carbon nanofiber fabrics may contribute to low-shear sliding [95], although their independent contribution to friction reduction was not

Just Accepted

quantified. These studies indicate that solid lubrication can operate either as a dominant mechanism or in combination with oil-mediated or mechanically reinforced nanofiber systems.

Although these studies demonstrated improved tribological performance, the experimental evidence for solid-lubricant transfer-film formation remains limited. In the core-shell system, FESEM confirmed the core-shell morphology, but the formation of a graphite transfer film was not directly examined [82]. In the MoS_2 containing system, SEM analysis showed reduced surface damage and improved fiber-network integrity after sliding, while FTIR and EDS provided evidence of PA6 material transfer between the contacting surfaces [94]. However, these results did not confirm the formation or composition of a MoS_2 containing transfer film. Similarly, Raman and HRTEM analyses identified graphitic structures within MWCNT/carbon nanofibers, but did not demonstrate their transfer to the counterface [95]. **Table. 4** summarizes the available characterization results and their limitations in evaluating transfer-film formation and behavior.

Just Accepted

Nanofiber system	Characterization methods and scope	Transfer-film composition	Coverage and continuity	Stability and evolution	Relationship with friction and wear	Evidence limitation	Ref.
Silicone-oil/PS core–shell fibers containing graphite	FESEM: Fiber morphology and core–shell structure Tribological tests: COF and wear rate	Graphite-containing shell identified Graphite transfer film not characterized	Transfer-film coverage and continuity not evaluated	Oil release and graphite transfer during sliding not directly monitored	COF and wear rate reduced by 70% and 50%, respectively, versus neat epoxy	Individual contributions of oil release and graphite lubrication not quantified Transfer-film formation unverified	[82]
MoS_2-containing F KM/PVDF nanofibers sliding against PA6/TPU	SEM: Surface damage and fiber integrity FTIR/EDS: PA6-related material transfer XPS: PA6/TPU interfacial composition and bonding	PA6 transfer supported by FTIR/EDS MoS_2-containing transfer-film composition not identified	Improved fiber-network integrity after sliding MoS_2 transfer-film coverage and continuity not quantified	Reduced material transfer after TPU modification Stable sliding operation over 44,000 cycles Dynamic film evolution not measured	Kinetic COF reduced by 41.4% improved sliding durability and reduced surface damage	PA6 material transfer verified but formation, phase, and stability of a MoS_2 low-shear transfer film not directly established	[94]
Hot-pressed MWCNT/carbon nanofibril fabrics	SEM: Fiber morphology Raman: Carbon structural characteristics HRTEM: Graphitic lamellae and crystallinity Tribological tests: COF and abrasive wear	Graphitic structures identified within the nanofibers Transferred carbon film not characterized	Counterface transfer-film coverage and continuity not evaluated	Sliding-induced transfer and film evolution not directly examined	Minimum COF of 0.15 and abrasive mass loss of 0.2 mg at 5 wt% MWCNT	Graphitic nanofiber structure confirmed but its transfer to the counterface and contribution to low-shear sliding not independently verified	[95]

Just Accepted

Table. 4 Experimental evidence and limitations of transfer-film formation in electrospun nanofiber systems.

The formation and properties of transfer films can affect friction and wear by changing the contact conditions at the sliding interface [84-87]. A continuous and stable film containing low-shear phases may reduce direct contact and interfacial shear resistance. In contrast, incomplete coverage, weak adhesion, or film removal during sliding may expose the underlying surfaces and increase friction and wear. Therefore, transfer-film composition, coverage, continuity, and stability should be considered together when evaluating lubrication performance. However, these relationships were not quantitatively established in the reviewed electrospun nanofiber systems. In particular, although EDS can identify transferred elements and their distribution on the sliding surface, elemental detection alone cannot establish the presence of a specific low-shear phase or demonstrate transfer-film continuity. Raman spectroscopy and XPS can provide information on the structural and chemical states of transferred materials, while TEM can further examine local film structure, thickness, and interfacial continuity. These analyses should be performed on the worn surfaces and counterfaces rather than only on the original nanofibers. Furthermore, characterization at different sliding stages is needed to evaluate film formation, removal, and regeneration. Such investigations would help establish clearer structure–property–tribological relationships between transfer-film characteristics and friction and wear performance.

4.2.4 Mechanical Reinforcement and Load-Bearing Effects

Mannarino et al. investigated the influence of the thermal curing conditions on the mechanical and tribological performance of electrospun nanofibers [80]. After thermal curing, interfiber junctions were formed (**Fig. 5(a)**), which enhanced the Young's modulus, yield stress, and toughness of the mat. Under the same conditions, the COF and wear rate were approximately two times and 10 times lower, respectively (**Fig. 5(b)** and (**c)**). The reduction in wear rate was interpreted as being correlated with the yield properties of the mat as well as with fiber breakage and abrasive wear occurring at the interfiber junctions during sliding contact. These results indicate that the low-friction performance and

Just Accepted

wear resistance of electrospun nanofiber mats can be improved through mechanical reinforcement and the load-supporting capacity of the fiber network without oil release or solid lubricant additives.

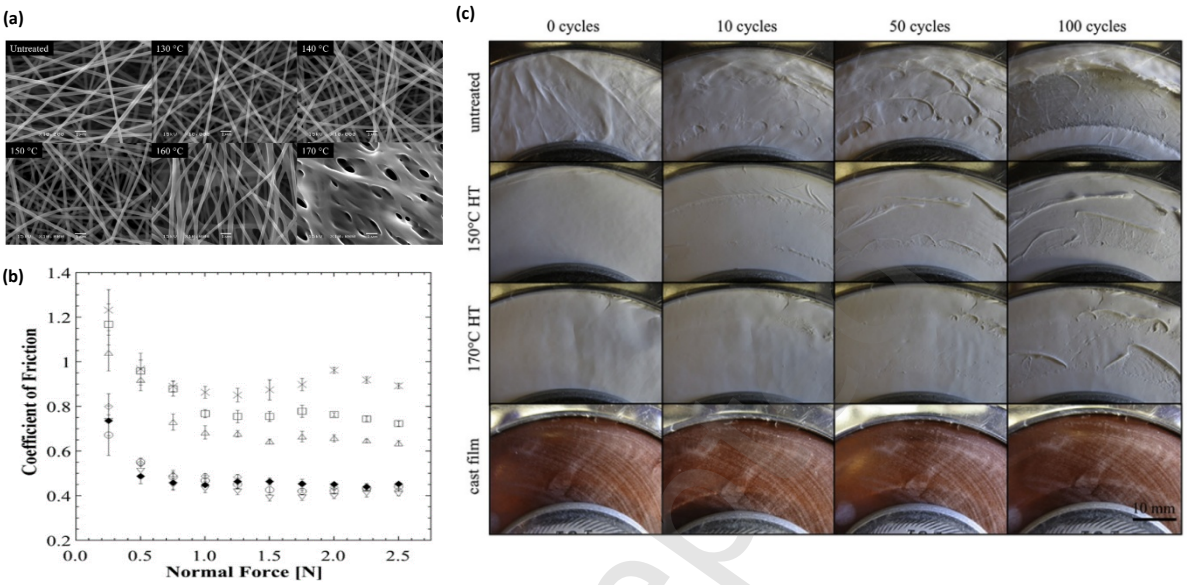


Fig. 5 (a) SEM micrographs of PA 6(3)T nanofibers after varying degrees of heat treatment. (b) COF of PA 6(3)T electrospun fiber mats as a function of normal force with varying heat-treatment temperatures: untreated (×), 130 °C (□), 140 °C (△), 150 °C (◇), 160 °C (▽), 170 °C (○), and cast film (◆). (c) Optical images of wear-track evolution in PA 6(3)T electrospun fiber mats with wear cycles and heat-treatment temperature.

Ali et al. prepared electrospun carbon-based nanofibers using polyacrylonitrile (PAN) as the carbon fiber precursor and subsequently fabricated a hot-pressed multi-walled carbon nanotube (MWCNT)/carbon nanofibril composite [95]. The authors first dispersed MWCNTs in a PAN solution and fabricated an MWCNT/PAN nanofibril composite fabric via electrospinning. After stabilization and carbonization, the PAN was converted into carbon-based nanofiber structures, resulting in the formation of a carbon nanofibril fabric containing MWCNTs. Hot pressing, which involves the simultaneous application of heat and static pressure, promotes closer interfiber contact and produces a denser and more stable fabric, while the incorporation of MWCNTs increased the tensile strength of the fabrics. Tribological testing showed that the COF decreased with increasing MWCNT content for the as-electrospun, stabilized, and carbonized fabrics (**Fig. 6**). In addition, the COF decreased with increasing normal force at relatively low loads and became approximately stable above 2 N,

Just Accepted

particularly for the stabilized and carbonized samples. The abrasive mass loss was also reduced by increasing the MWCNT content and by hot pressing. These results indicate that densification and mechanical reinforcement of the nanofiber network are associated with improved structural stability and wear resistance under mechanical loading. HRTEM and Raman analyses also confirmed the formation of graphitic structures after heat treatment, which may additionally contribute to low-shear lubrication; however, the specific contribution of this graphitic phase to friction reduction was not independently evaluated.

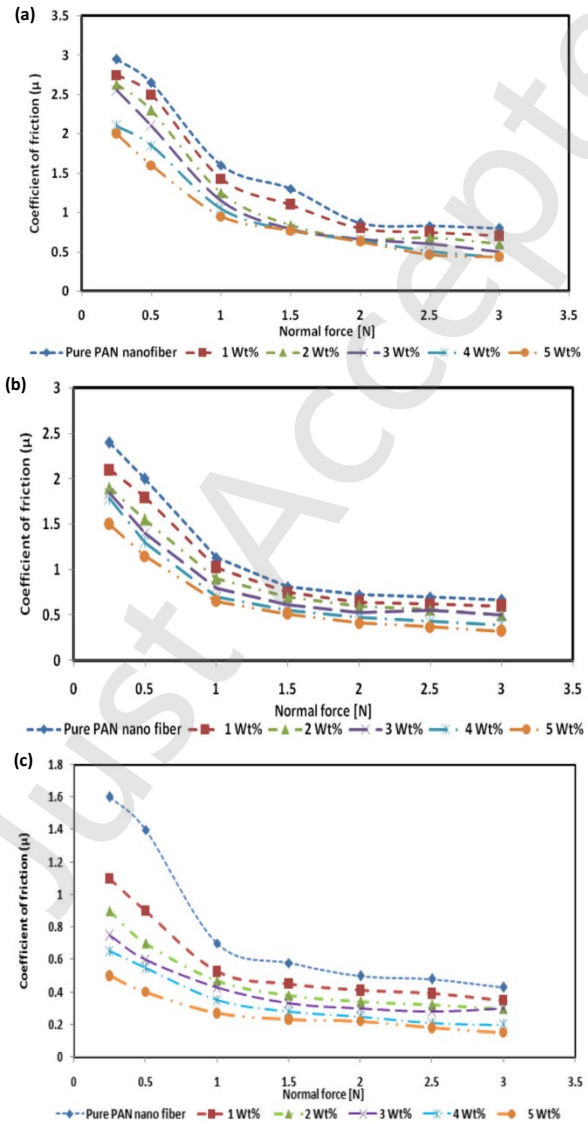


Fig. 6 COF of the MWCNT/PAN fabrics with various MWCNT contents as a function of normal force: (a) as-electrospun, (b) stabilized, and (c) carbonized fabrics.

Just Accepted

To further compare the effects of mechanical reinforcement on tribological performance, **Table. 5** summarizes the reported mechanical properties, contact conditions, friction and wear results, and post-sliding structural damage of the nanofiber systems [80,95]. In PA 6(3)T nanofiber mats, the wear rate was found to be consistent with a modified Ratner-Lancaster model incorporating the yield properties of the mats [80]. In addition, post-wear observations showed deformation and severe material loss in untreated mats, whereas annealed mats exhibited delayed tearing and delamination during repeated abrasive contact. These results support the contribution of improved mechanical stability to wear resistance. In MWCNT/carbon nanofiber fabrics, mechanical reinforcement and reduced friction and wear were reported together, although the individual contributions of increased stiffness, structural densification, and graphitic lubrication were not independently determined [95]. Furthermore, the effects of these structural changes may vary with contact load and sliding conditions.

Mechanical load-bearing effects should be distinguished from interfacial friction-reduction mechanisms. Increased stiffness and stronger interfiber junctions may improve resistance to deformation, fiber breakage, and structural degradation, whereas low-shear interfacial lubrication can reduce shear resistance between contacting surfaces. Therefore, improved wear resistance resulting from mechanical reinforcement does not necessarily demonstrate a low-shear lubrication mechanism. In addition, structural reinforcement involves potential trade-offs. For example, thermal annealing can improve mechanical properties and wear resistance while reducing the porosity of nanofiber mats [80]. Such structural densification may also restrict lubricant storage and transport in oil-containing systems, although this effect was not directly evaluated in these studies. Further comparisons of mechanical properties, post-sliding failure modes, and tribological performance under controlled contact conditions are needed to clarify these relationships.

Just Accepted

Structural modification	Mechanical properties	Contact conditions	Quantitative tribological response	Mechanical property–tribological relationship	Ref.
Thermal annealing of PA 6(3)T mats	Young's modulus, yield stress, and toughness	Friction: variable normal loads, with COF approximately constant above 1 N for mats annealed at ≥150 °C	At 25 g: COF 1.23 → 0.67	Increased mechanical properties were accompanied by lower friction and wear	[80]
Formation of stronger interfiber junctions	increased approximately 2–10-fold	Abrasion: 100 g load, 10–100 cycles for structural observations	Wear rate reduced by approximately 90%	Wear rate was correlated with yield properties	
MWCNT incorporation, carbonization, and hot pressing of PAN-derived carbon nanofibril fabrics	Tensile strength increased from approximately 40 to 60 Mpa modulus of hot-pressed fabrics approximately 3–4 Gpa	Friction evaluated under varying normal loads Abrasive wear evaluated separately over repeated cycles	Minimum COF approximately 0.15 Minimum reported abrasive mass loss approximately 0.2 mg	Mechanical strengthening and structural modification were associated with reduced friction and abrasive wear, but the individual contributions were not quantified	[95]

Post-sliding damage	Mechanical load-bearing effect	Interfacial friction-reduction mechanism	Structural trade-off and limitation	Ref.
Untreated mats showed deformation and wear after 10 cycles and severe material loss before 100 cycles	Stronger interfiber junctions and improved yield resistance contribute to reduced deformation, fiber breakage, and abrasive wear	No additional low-shear lubricant was introduced.	Improved mechanical properties and wear resistance accompanied by reduced porosity.	[80]
Annealed mats showed delayed tearing and delamination		Friction reduction was associated with structural modification rather than a separately verified lubricating film.	Individual effects of stiffness and interfiber bonding were not isolated	
Delamination and brittle fracture were reported with increasing MWCNT content	Increased strength and stiffness may improve resistance to deformation and mechanical damage	Graphitic structures may contribute to low-shear sliding, but their transfer to the interface and independent lubricating contribution were not verified	Excessive MWCNT incorporation may promote brittleness and delamination.	[95]
Post-sliding fiber collapse and pullout were not independently quantified			Mechanical reinforcement and graphitic lubrication effects were not separated.	

Table. 5. Relationships between mechanical properties, contact conditions, structural damage, and tribological performance in mechanically reinforced electrospun nanofiber systems.

Just Accepted

Overall, the studies discussed in Sections 4.1 and 4.2 show that the structural properties of electrospun nanofibers play an important role in determining their friction and wear behavior. In oil-mediated systems, fiber morphology, network structure, and thickener concentration affect oil structuring and tribological performance [17, 21, 22, 25, 90, 91]. For example, smooth cellulose acetate butyrate fibers showed a lower COF (0.089) and smaller wear scar diameter (305 μm) than porous fibers (0.119 and 652 μm) [22]. These results indicate that a porous morphology does not necessarily provide better lubrication. Differences in lubricant supply to the contact surface may contribute to this behavior, although their contribution was not independently quantified. In addition, increasing the cellulose acetate propionate thickener concentration from 3 to 6 wt% increased the COF from 0.084 to 0.099, while decreasing the wear scar diameter from 445 to 378 μm [90]. These results indicate that friction reduction and wear resistance do not always improve simultaneously and depend on the structural characteristics of the nanofiber network.

In non-oil systems, surface modification and mechanical reinforcement also affect friction and wear behavior. MPC grafting reduced the COF of PCL nanofibers by approximately 65% [20], while CNT incorporation reduced the COF of PVDF nanofibers by 14.4%, together with improved wettability and Ca^{2+} adsorption [93]. Furthermore, thermal annealing of PA 6(3)T nanofiber mats reduced the COF by 45.5% and the wear rate by 90.0% under a 25 g load [80]. Although thermal annealing improved the mechanical properties and wear resistance, it also reduced the porosity of the nanofiber mats, indicating a trade-off between structural reinforcement and porosity. In addition, the combination of interfacial crosslinking and MoS_2 lubrication reduced friction and improved sliding durability, suggesting that mechanical reinforcement and solid lubrication can provide complementary benefits [94].

These findings indicate that the structural design of electrospun nanofibers should consider both lubrication performance and mechanical stability. Improvements in one property do not necessarily lead to improvements in all tribological properties, and trade-offs may occur between oil retention and lubricant supply, friction reduction and wear resistance, or mechanical strength and porosity. However,

Just Accepted

the individual effects of fiber diameter, pore structure, fiber alignment, and core–shell integrity have not been fully quantified because multiple structural and compositional parameters were often changed simultaneously. **Table. 6** summarizes the reported quantitative tribological results and their relationships with structural properties, together with the key lubrication mechanisms, potential complementary effects, design trade-offs, available experimental evidence, current research limitations, and unresolved scientific questions.

Just Accepted

Lubrication category	Structural parameter / modification	Key lubrication mechanism	Quantitative tribological response	Structure–property–tribological relationship	Synergistic or complementary effect	Trade-off	Available experimental evidence	Current research limitation	Unresolved scientific question	Ref
Core–shell oil-mediated	Silicone-oil core and graphite-containing PS sh ell	Oil release following shell damage graphite-mediated solid lubrication	COF reduction: ~70% Wear rate reduction: ~50% vs neat epoxy	Core–shell incorporation is associated with reduced friction and wear, potentially through oil release and graphite lubrication	Potential combined silicone-oil and graphite lubrication	Premature shell damage may limit lubricant supply	Core–shell morphology friction and wear tests	OI release kinetics and individual lubricant contributions not quantified	How do shell integrity and oil release rate affect long-term lubrication?	[82]
	LSL/PVP composition and fiber concentration	Oil immobilization within an entangled fiber network	COF: 0.135 to 0.093 Wear scar: 362 to 346 μm (70:30, 10–20 wt%)	Increased fiber content strengthens oil structuring and is associated with reduced friction and wear	Improved oil structuring with increased network formation	Stronger oil immobilization may restrict replenishment	Composition-dependent rheological and tribological results	Lubricant transport during sliding not directly measured	How does network density affect oil replenishment and friction stability?	[91]
	LSL/EC ratio and fiber concentration	Formation of a grease-like network retaining oil	COF: 0.094 to 0.082 Wear scar: 359 to 208 μm (70:30, 10–30 wt%)	Increased nanofiber concentration enhances gel-like properties and is associated with improved wear resistance	Enhanced gel formation and improved wear resistance	No quantitative trade-off established	Concentration-dependent rheology and wear measurements	Oil retention and interfacial supply not independently evaluated	What network structure provides sufficient oil retention and supply?	[21]
	Electrospun EC web vs thermogelated EC	Physical oil structuring by interconnected EC fibers	COF: 0.110 to 0.075 Wear scar: 433.1 to 359.7 μm (15 wt%)	Electrospun network formation modifies oil rheology and improves friction and wear performance	Electrospun network improves oil structuring and tribological behavior	No quantitative trade-off established	Structural, rheological, and friction/wear comparisons	Network evolution during sliding not characterized	How does fiber-network integrity influence prolonged lubrication?	[17]
Oil structuring	Smooth vs porous CAb fibers	Morphology-dependent oil retention and lubricant availability	COF: 0.089 vs. 0.119 Wear scar: 305 vs. 652 μm (5 wt%)	Porous morphology changes oil retention, while smooth fibers exhibit lower friction and wear	No independent synergistic effect established	Porous fibers may retain oil more strongly but exhibit higher friction and wear	Fiber morphology, oil-retention behavior, and tribological tests	Effects of porosity and other morphological changes not isolated	How does pore structure control oil retention versus interfacial replenishment?	[22]
	CAp thickener concentration	Concentration-dependent oil thickening and structuring	COF: 0.084 to 0.099 Wear scar: 445 to 378 μm (3–6 wt%)	Increased thickener concentration is associated with higher friction but reduced wear	Improved wear protection with increased thickener concentration	Higher concentration reduces wear but increases COF	Rheological, friction, and wear measurements	Interfacial lubricant distribution not directly measured	What thickener concentration gives the best friction–wear balance?	[90]
	LSL/PCL composition and fiber morphology	Composition-dependent oil structuring and mechanical resistance	COF: 0.11–0.18 Wear diameter: 440–860 μm	Increased structural stiffness is associated with higher friction and wear	No independent synergistic effect established	Increased network stiffness is associated with higher friction and wear	Fiber morphology, mechanical/rheological properties, and tribological results	Composition and morphology effects not independently separated	How do fiber stiffness and morphology individually influence lubrication?	[25]
Hydration	MPC grafting onto PCL nanofibers	Zwitterionic-group-associated hydration lubrication	COF reduction: ~55% vs pure PCL	MPC grafting improves hydration-associated surface properties and reduces friction	Hydration lubrication supported by the fibrous membrane	No quantitative trade-off established	Surface functionalization, WCA, and water-dependent friction	Hydration layer not directly observed during sliding	How does hydration-layer stability change under applied load and shear?	[20]
	PMPC/PCL composition and fabrication humidity	PMPC-associated surface hydration and low-shear interfacial behavior	COF: ~0.12 at 20% RH below 0.05 at higher RH	Changes in fabrication humidity and polymer composition influence surface hydration and friction	Surface hydration and morphology contribute to low friction	No quantitative trade-off established	SEM/EDS, TGA/DTG bound-water-related signals, and friction tests	Hydration-layer continuity under sliding not directly verified	How do surface PMPC distribution and hydration-layer continuity affect friction?	[92]
	PMPC nanoskin on PLA fibers	Hydration-associated lubrication by surface PMPC groups	COF below 0.025 ~16-fold lower than original fibers stable for 12,000 cycles	Robust PMPC modification is associated with reduced friction and improved sliding durability	Hydration-associated lubrication combined with robust surface anchoring	No quantitative trade-off established	SEM/XPS, surface wettability, and repeated sliding tests	Hydration layer not directly monitored	Does the hydration layer remain intact throughout repeated sliding?	[33]
	Lecithin content in PLA fibers	Hydration associated with zwitterionic lecithin head groups	Minimum COF: ~0.112 (20% lecithin)	Increased lecithin content enhances bound-water characteristics and is associated with lower friction	Lecithin incorporation improves bound-water characteristics and lubrication	No quantitative trade-off established	SEM, WCA, TGA, and friction measurements	Interfacial hydration not directly measured	How much does hydration contribute relative to changes in fiber morphology?	[24]
Ion-mediated	CNT-modified PVDF and Ca^{2+} adsorption	Proposed lubrication associated with adsorbed Ca^{2+} and its hydration	COF: 0.14 to 0.12 Reduction: 14.4% vs PVDF	CNT incorporation improves wettability and Ca^{2+} adsorption while reducing friction	Wettability improvement and ion adsorption accompany friction reduction	No quantitative trade-off established	Surface characterization, Ca^{2+} adsorption, and friction tests	Contribution of Ca^{2+}-associated hydration not distinguished from other surface effects	Does adsorbed Ca^{2+} directly contribute to low-shear interfacial lubrication?	[93]
Solid lubrication	MoS_2 nanosheets and interfacial crosslinking	MoS_2-associated low-shear lubrication with structural stabilization	Kinetic COF reduction: 41.4% Stable for 44,000 sliding cycles	MoS_2 incorporation reduces friction, while interfacial crosslinking contributes to structural durability	Interfacial reinforcement and MoS_2 lubrication provide complementary functions	Crosslinking alone is insufficient to prevent severe sliding wear	MoS_2 incorporation, crosslinked structure, and sliding durability tests	Individual effects of MoS_2 and crosslinking not quantified	How much does each component contribute to friction reduction and durability?	[94]
Mechanical reinforcement	Thermal annealing and interfiber junctions	Interfiber bonding and improved load-bearing stability	COF: 1.23 to 0.67 Wear rate: 6.38×10^{-5} to 6.40×10^{-7} g/(cm (2 5 g)	Interfiber bonding improves mechanical properties and wear resistance while reducing porosity	Interfiber bonding improves mechanical strength and wear resistance	Annealing enhances mechanical properties while reducing porosity	Structural, mechanical, friction, and wear measurements	Effects of porosity and interfiber bonding not independently isolated	What degree of interfiber bonding optimizes wear resistance while preserving porosity?	[80]
	MWCNT incorporation and hot pressing	Mechanical reinforcement and proposed graphitic lubrication	Minimum COF: 0.15 Abrasive mass loss: 0.2 mg (5 wt% MWCNT)	Reinforcement and densification improve mechanical properties and are associated with lower friction and abrasive loss	Potential mechanical reinforcement and graphitic lubrication	No quantitative trade-off established	MWCNT incorporation, structural/mechanical tests, friction and abrasive-wear measurements	Effects of MWCNT and hot pressing not separated	How do reinforcement, densification, and carbonaceous lubrication individually affect wear?	[95]

Table. 6 Critical comparison of lubrication mechanisms, tribological performance, and research gaps in electrospun nanofiber systems.

5. Limitations and Future Perspectives

Despite the promising tribological performance of electrospun nanofiber systems, several limitations remain. Direct quantitative comparison among reported studies is still difficult because tribological test conditions, including counterface materials, applied loads, sliding speeds, contact geometries, and lubrication environments, vary substantially. In addition, some proposed lubrication mechanisms are mainly inferred from friction and wear behavior rather than directly verified under actual sliding conditions. Long-term structural durability, reproducibility, and maintenance of functional components during repeated sliding also remain important challenges for practical applications. Therefore, future studies should focus on more standardized tribological evaluation and reporting, direct interfacial characterization during or after sliding, and improved structural stability and reproducible fabrication of electrospun nanofiber systems. These efforts will help establish more reliable structure–mechanism–performance relationships and support the practical application of electrospun nanofibers in tribological systems.

6. Conclusions

Electrospun nanofibers have emerged as a versatile class of materials capable of overcoming the inherent trade-off between friction reduction and mechanical durability. Rather than acting as mere passive supports, these nanofibrous structures are multifunctional platforms where structural morphology, surface chemistry, and lubricant integration converge to dictate the interfacial tribological behavior. Overall, the reviewed studies demonstrate that the tribological performance of electrospun nanofibers is governed by the interplay between nanofiber architecture, interfacial chemistry, and the dominant lubrication pathway.

The central principle governing these systems relies on precise tailoring of the nanofiber network to manipulate the interfacial shear and load support. Oil-mediated systems capitalize on the high porosity and core-shell architecture of nanofibers to enable controlled liquid release and oil-structuring effects,

Just Accepted

which can be further augmented by synergistic solid lubricant. By contrast, non-oil strategies achieve low-friction interfaces through intrinsic chemical and structural engineering. This is accomplished by using zwitterionic or hydrophilic hydration layers to create fluid-like, low-shear interfaces or by employing thermal curing, carbonization, and hot-pressing to construct robust load-bearing networks that suppress wear.

Ultimately, optimizing low-friction performance requires moving beyond a single-material mindset to embrace a holistic design strategy that harmonizes the fiber diameter, alignment, internal architecture, and surface potential. To transition these advanced nanofibrous coatings from laboratory innovations to practical industrial and biological applications, including self-lubricating surfaces, anti-adhesion biomembranes, and wear-resistant composites, future research must bridge the key technical gaps. Priority should be given to establishing quantitative structure–property–performance relationships, ensuring long-term structural integrity under repeated high-load sliding, and conducting in-depth post-wear interfacial characterization. Addressing these foundational challenges will position electrospun nanofibers among the leading material platforms for next-generation tribological engineering.

Acknowledgements

This work was supported by the National Research Foundation of Korea (NRF) grant (RS-2025-02309062).

Availability of data and materials

Not applicable.

Competing interests

The authors have no competing interests to declare that are relevant to the content of this article.

Just Accepted

References

[1] Luo J, Zhou X. Superlubricitive engineering—Future industry nearly getting rid of wear and frictional energy consumption. *Friction* **8**(4): 643–665 (2020). https://doi.org/10.1007/s40544-020-0393-0.

[2] Asnida M, Hisham S, Awang N, Amirruddin A, Noor M, Kadirgama K, Ramasamy D, Najafi G, Tarlochan F. Copper (II) oxide nanoparticles as additive in engine oil to increase the durability of piston-liner contact. *Fuel* **212**: 656–667 (2018). https://doi.org/10.1016/j.fuel.2017.10.002.

[3] Borrego M, Kuhn E, Martín-Alfonso J E, Franco J M. Assessment of the tribological performance of electrospun lignin nanofibrous web-thickened bio-based greases in a nanotribometer. *Nanomaterials* **13**(21): 2852 (2023). https://doi.org/10.3390/nano13212852.

[4] Huang J, Tan J, Fang H, Gong F, Wang J. Tribological and wear performances of graphene-oil nanofluid under industrial high-speed rotation. *Tribol Int* **135**: 112–120 (2019). https://doi.org/10.1016/j.triboint.2019.02.041.

[5] Iioka M, Kawanabe W, Tsujimura S, Kobayashi T, Shohji I. An evaluation of the wear resistance of electroplated nickel coatings composited with 2, 2, 6, 6-tetramethylpiperidine 1-oxyl-oxidized cellulose nanofibers. *Polymers* **16**(2): 224 (2024). https://doi.org/10.3390/polym16020224.

[6] Jia X, Huang J, Li Y, Yang J, Song H. Monodisperse Cu nanoparticles@ MoS_2 nanosheets as a lubricant additive for improved tribological properties. *Appl Surf Sci* **494**: 430–439 (2019). https://doi.org/10.1016/j.apsusc.2019.07.194.

[7] Jia Z, Wang Z, Liu C, Zhao L, Ni J, Li Y, Shao X, Wang C. The synthesis and tribological properties of Ag/polydopamine nanocomposites as additives in poly-alpha-olefin. *Tribol Int* **114**: 282–289 (2017). https://doi.org/10.1016/j.triboint.2017.04.039

[8] Kotia A, Ghosh G K, Srivastava I, Deval P, Ghosh S K. Mechanism for improvement of friction/wear by using Al_2O_3 and SiO_2/Gear oil nanolubricants. *J Alloys Compd* **782**: 592–599 (2019). https://doi.org/10.1016/j.jallcom.2018.12.215.

[9] Nan F, Wang D. Tribological properties of attapulgite nanofiber as lubricant additive for electric-brush plated Ni coating. *Lubricants* **11**(5): 204 (2023). https://doi.org/10.3390/lubricants11050204.

[10] Toro-Gallego M, Valencia C, Sánchez M C, Martín-Alfonso J E, Franco J M. Use of electrospun cellulose acetate/silica composites as multifunctional ingredients in eco-friendly semisolid lubricant formulations. *J Appl Polym Sci* **142**(7): e56489 (2025). https://doi.org/10.1002/app.56489.

Just Accepted

[11] Wang Y, Wan Z, Lu L, Zhang Z, Tang Y. Friction and wear mechanisms of castor oil with addition of hexagonal boron nitride nanoparticles. *Tribol Int* **124**: 10–22 (2018). https://doi.org/10.1016/j.triboint.2018.03.035.

[12] Zhai W, Lu W, Liu X, Zhou L. Nanodiamond as an effective additive in oil to dramatically reduce friction and wear for fretting steel/copper interfaces. *Tribol Int* **129**: 75–81 (2019). https://doi.org/10.1016/j.triboint.2018.08.006.

[13] Cho Y, Baek J W, Sagong M, Ahn S, Nam J S, Kim I D. Electrospinning and nanofiber technology: fundamentals, innovations, and applications. *Adv Mater* **37**(28): 2500162 (2025). https://doi.org/10.1002/adma.202500162.

[14] Ahmadi Bonakdar M, Rodrigue D. Electrospinning: processes, structures, and materials. *Macromol* **4**(1): 58–103 (2024). https://doi.org/10.3390/macromol4010004.

[15] Al-Abduljabbar A, Farooq I. Electrospun polymer nanofibers: processing, properties, and applications. *Polymers* **15**(1): 65 (2022). https://doi.org/10.3390/polym15010065.

[16] Kamaraj M, Moghimi N, Chen J, Morales R, Chen S, Khademhosseini A, John J V. New dimensions of electrospun nanofiber material designs for biotechnological uses. *Trends Biotechnol* **42**(5): 631–647 (2024). https://doi.org/10.1016/j.tibtech.2023.11.008.

[17] Borrego M, Martín-Alfonso J, Valencia C, Sánchez Carrillo M C, Franco J. Developing electrospun ethylcellulose nanofibrous webs: An alternative approach for structuring castor oil. *ACS Appl Polym Mater* **4**(10): 7217–7227 (2022). https://doi.org/10.1021/acsapm.2c01090.

[18] Chen Q, Yan X, Chen K, Feng C, Wang D, Li X, Zhao X, Chai Z, Wang Q, Zhang D. Electrospun fibrous membrane reinforced hydrogels with preferable mechanical and tribological performance as cartilage substitutes. *J Mater Chem B* **11**(8): 1713–1724 (2023). https://doi.org/10.1039/D2TB02511F.

[19] Li J, Gao L, Xu R, Ma S, Ma Z, Liu Y, Wu Y, Feng L, Cai M, Zhou F. Fibers reinforced composite hydrogels with improved lubrication and load-bearing capacity. *Friction* **10**(1): 54–67 (2022). https://doi.org/10.1007/s40544-020-0389-9.

[20] Cheng L, Wang Y, Sun G, Wen S, Deng L, Zhang H, Cui W. Hydration-enhanced lubricating electrospun nanofibrous membranes prevent tissue adhesion. *Research* **2020**: 4907185 (2020). https://doi.org/10.34133/2020/4907185.

[21] Borrego M, Martín-Alfonso J E, Valencia C, Sánchez M C, Franco J M. Impact of the morphology of electrospun lignin/ethylcellulose nanostructures on their capacity to thicken castor oil. *Polymers* **14**(21): 4741 (2022). https://doi.org/10.3390/polym14214741.

Just Accepted

[22] Martín-Alfonso M A, Rubio-Valle J F, Martín-Alfonso J E, Franco J M. Oleodispersions of electrospun cellulose acetate butyrate nanostructures: toward renewable semisolid lubricants. *Adv Sustain Syst* **8**(7): 2300592 (2024). https://doi.org/10.1002/adsu.202300592.

[23] Zhang X, Chen Q, Chen K, Feng H, Feng C, Li X, Zhang D, Ge S. Tough, slippery, and low-permeability multilayer hydrogels modified by anisotropic fiber membrane for soft tissue replacement. *ACS Appl Mater Interfaces* **16**(36): 47314–47324 (2024). https://doi.org/10.1021/acsami.4c11080.

[24] Li J, Lin H, Li J, Wang Y. Engineered lubricative lecithin-based electrospun nanofibers for the prevention of postoperative abdominal adhesion. *Pharmaceutics* **16**(12): 1562 (2024). https://doi.org/10.3390/pharmaceutics16121562.

[25] Rubio-Valle J F, Valencia C, Estrada-Villegas G M, Martín-Alfonso J E, Franco J M. Exploration of low-sulfonate lignin electrospinning conditions for the development of new renewable lubricant formulations. *Nanoscale* **17**(5): 2728–2741 (2025). https://doi.org/10.1039/D4NR04426F.

[26] Al-Dhahebi A M, Ling J, Krishnan S G, Yousefzadeh M, Elumalai N K, Saheed M S M, Ramakrishna S, Jose R. Electrospinning research and products: The road and the way forward. *Appl Phys Rev* **9**(1): 011319 (2022). https://doi.org/10.1063/5.0077959.

[27] Wang Q, Ji P, Bu T, Mao Y, He H, Ge N. Recent progress in the application of electrospinning technology in the biomedical field. *J Funct Biomater* **16**(7): 266 (2025). https://doi.org/10.3390/jfb16070266.

[28] Reddy V S, Tian Y, Zhang C, Ye Z, Roy K, Chinnappan A, Ramakrishna S, Liu W, Ghosh R. A review on electrospun nanofibers based advanced applications: From health care to energy devices. *Polymers* **13**(21): 3746 (2021). https://doi.org/10.3390/polym13213746.

[29] Zheng Q, Xi Y, Weng Y. Functional electrospun nanofibers: Fabrication, properties, and applications in wound-healing process. *RSC Adv* **14**(5): 3359–3378 (2024). https://doi.org/10.1039/D3RA07075A.

[30] Zhao Y-S, Huang J, Yang X, Wang W, Yu D-G, He H, Liu P, Du K. Electrospun nanofibers and their application as sensors for healthcare. *Front Bioeng Biotechnol* **13**: 1533367 (2025). https://doi.org/10.3389/fbioe.2025.1533367.

[31] Aflaha R, Putri L A, Farrel A, Anzinger S, Rianjanu A, Yulianto N, Fueldner M, Roto R, Peiner E, Wasisto H S. Crafting high-temperature stable and hydrophobic nanofiber membranes for particulate matter filtration. *Commun Mater* **6**(1): 87 (2025). https://doi.org/10.1038/s43246-025-00799-y.

[32] Ma S, Li A, Pan L. Application progress of multifunctional polymer composite nanofibers based on electrospinning: A brief review. *Polymers* **16**(17): 2459 (2024). https://doi.org/10.3390/polym16172459.

Just Accepted

[33] Wang Y, Xu Y, Zhai W, Zhang Z, Liu Y, Cheng S, Zhang H. In-situ growth of robust superlubricated nano-skin on electrospun nanofibers for post-operative adhesion prevention. *Nat Commun* **13**(1): 5056 (2022). https://doi.org/10.1038/s41467-022-32804-0.

[34] Souza Plath A M, Alinezhadfar M, Ferguson S J. Friction and wear characterizations in electrospun nanofibrous scaffolds for cartilage engineering. *Nano Select* **6**(7): e202400165 (2025). https://doi.org/10.1002/nano.202400165.

[35] Ji D, Lin Y, Guo X, Ramasubramanian B, Wang R, Radacsi N, Jose R, Qin X, Ramakrishna S. Electrospinning of nanofibres. *Nat Rev Methods Primers* **4**(1): 1 (2024). https://doi.org/10.1038/s43586-023-00278-z.

[36] Wang C, Wang W, Qi H, Dai Y, Jiang S, Ding B, Wang X, Li C, Zeng J, Wu T. Electrospinning and electrospun nanofibers: From academic research to industrial production. *Prog Mater Sci* **154**: 101494 (2025). https://doi.org/10.1016/j.pmatsci.2025.101494.

[37] Shaban M, Mosa T M, Abdel-Hamid H, Abdalfarg N, Hashim G. Advancements in electrospinning: a comprehensive review of historical development, key parameters, applications, and challenges. *Discover Chem* **3**(1): 82 (2026). https://doi.org/10.1007/s44371-026-00539-2.

[38] Nadaf A, Gupta A, Hasan N, Ahmad S, Kesharwani P, Ahmad F J. Recent update on electrospinning and electrospun nanofibers: current trends and their applications. *RSC Adv* **12**(37): 23808–23828 (2022). https://doi.org/10.1039/D2RA02864F.

[39] Han W-H, Wang M-Q, Yuan J-X, Hao C-C, Li C-J, Long Y-Z, Ramakrishna S. Electrospun aligned nanofibers: A review. *Arab J Chem* **15**(11): 104193 (2022). https://doi.org/10.1016/j.arabjc.2022.104193.

[40] Chinnappan B A, Krishnaswamy M, Xu H, Hoque M E. Electrospinning of biomedical nanofibers/nanomembranes: effects of process parameters. *Polymers* **14**(18): 3719 (2022). https://doi.org/10.3390/polym14183719.

[41] Abdulhussain R, Adebisi A, Conway B R, Asare-Addo K. Electrospun nanofibers: Exploring process parameters, polymer selection, and recent applications in pharmaceuticals and drug delivery. *J Drug Deliv Sci Technol* **90**: 105156 (2023). https://doi.org/10.1016/j.jddst.2023.105156.

[42] Rajabifar N, Rostami A, Afshar S, Mosallanezhad P, Zarrintaj P, Shahrousvand M, Nazockdast H. Wound dressing with electrospun core-shell nanofibers: from material selection to synthesis. *Polymers* **16**(17): 2526 (2024). https://doi.org/10.3390/polym16172526.

[43] Zhao J, Chen L, Ma A, Bai X, Zeng Y, Liu D, Liu B, Zhang W, Tang S. Recent advances in coaxial electrospun nanofibers for wound healing. *Mater Today Bio* **29**: 101309 (2024). https://doi.org/10.1016/j.mtbio.2024.101309.

Just Accepted

[44] Akhila B, Abhijith V, Sreedharan M, Ravindran L, Sathian A, Thomas S, Sadasivan S M. Innovations in core–shell electrospinning: a comprehensive review in recent advances of core–shell electrospun polylactic acid nanocomposite fibers for potential biomedical applications. *ACS Biomater Sci Eng* **11**(7): 3826–3857 (2025). https://doi.org/10.1021/acsbiomaterials.5c00194.

[45] Yan K, Le Y, Mengen H, Zhongbo L, Zhulin H. Effect of solution miscibility on the morphology of coaxial electrospun cellulose acetate nanofibers. *Polymers* **13**(24): 4419 (2021). https://doi.org/10.3390/polym13244419.

[46] Rathore P, Schiffman J D. Beyond the single-nozzle: Coaxial electrospinning enables innovative nanofiber chemistries, geometries, and applications. *ACS Appl Mater Interfaces* **13**(1): 48–66 (2020). https://doi.org/10.1021/acsami.0c17706.

[47] Kanaan A F, de Oliveira W A, Boaron C K, Sauer H, Santana M A, Piedade A P, Vidotti M. Electrospinning technology applied for building up electrochemical platforms–a review. *J Solid State Electrochem*: (2026). https://doi.org/10.1007/s10008-026-06625-w.

[48] Taokaew S, Chuenkaek T. Developments of core/shell chitosan-based nanofibers by electrospinning techniques: a review. *Fibers* **12**(3): 26 (2024). https://doi.org/10.3390/fib12030026.

[49] Han D, Steckl A J. Coaxial electrospinning formation of complex polymer fibers and their applications. *ChemPlusChem* **84**(10): 1453–1497 (2019). https://doi.org/10.1002/cplu.201900281.

[50] Vats S, Anyfantakis M, Honaker L W, Basoli F, Lagerwall J P. Stable Electrospinning of core-functionalized coaxial fibers enabled by the minimum-energy interface given by partial core–sheath miscibility. *Langmuir* **37**(45): 13265–13277 (2021). https://doi.org/10.1021/acs.langmuir.1c01824.

[51] Li M, Zheng Y, Xin B, Xu Y. Coaxial electrospinning: jet motion, core–shell fiber morphology, and structure as a function of material parameters. *Ind Eng Chem Res* **59**(13): 6301–6308 (2020). https://doi.org/10.1021/acs.iecr.9b05866.

[52] Zhang R, Chen X, Wang H, Sun J, Huang S, Zhang X, Long J. Study on deposition of coaxial electrospinning fibers by coaxial auxiliary flow field. *Polymers* **17**(3): 396 (2025). https://doi.org/10.3390/polym17030396.

[53] Kaerkitcha N, Chuangchote S, Hachiya K, Sagawa T. Influence of the viscosity ratio of polyacrylonitrile/poly (methyl methacrylate) solutions on core–shell fibers prepared by coaxial electrospinning. *Polym J* **49**(6): 497–502 (2017). https://doi.org/10.1038/pj.2017.8.

[54] Pant B, Park M, Park S-J. Drug delivery applications of core-sheath nanofibers prepared by coaxial electrospinning: A review. *Pharmaceutics* **11**(7): 305 (2019). https://doi.org/10.3390/pharmaceutics11070305.

Just Accepted

[55] Rahmani S, Arefazar A, Latifi M. PMMA/PS coaxial electrospinning: core–shell fiber morphology as a function of material parameters. *Mater Res Express* **4**(3): 035304 (2017). https://doi.org/10.1088/2053-1591/aa600c.

[56] Wang M, Wang K, Yang Y, Liu Y, Yu D-G. Electrospun environment remediation nanofibers using unspinnable liquids as the sheath fluids: A review. *Polymers* **12**(1): 103 (2020). https://doi.org/10.3390/polym12010103.

[57] Ning T, Zhou Y, Xu H, Guo S, Wang K, Yu D-G. Orodispersible membranes from a modified coaxial electrospinning for fast dissolution of diclofenac sodium. *Membranes* **11**(11): 802 (2021). https://doi.org/10.3390/membranes11110802.

[58] Chen X, Liu Y, Liu P. Electrospun core–sheath nanofibers with a cellulose acetate coating for the synergistic release of zinc ion and drugs. *Mol Pharm* **21**(1): 173–182 (2023). https://doi.org/10.1021/acs.molpharmaceut.3c00703.

[59] Zhu J, Huang W, Zhang Q, Ling S, Chen Y, Kaplan D L. Aqueous-based coaxial electrospinning of genetically engineered silk elastin core-shell nanofibers. *Materials* **9**(4): 221 (2016). https://doi.org/10.3390/ma9040221.

[60] Xue J, Wu T, Dai Y, Xia Y. Electrospinning and electrospun nanofibers: methods, materials, and applications. *Chem Rev* **119**(8): 5298–5415 (2019). https://doi.org/10.1021/acs.chemrev.8b00593.

[61] Nguyen T D, Roh S, Nguyen M T N, Lee J S. Structural control of nanofibers according to electrospinning process conditions and their applications. *Micromachines* **14**(11): 2022 (2023). https://doi.org/10.3390/mi14112022.

[62] Wang P, Lv H, Cao X, Liu Y, Yu D-G. Recent progress of the preparation and application of electrospun porous nanofibers. *Polymers* **15**(4): 921 (2023). https://doi.org/10.3390/polym15040921.

[63] Zhou Y, Liu Y, Zhang M, Feng Z, Yu D-G, Wang K. Electrospun nanofiber membranes for air filtration: A review. *Nanomaterials* **12**(7): 1077 (2022). https://doi.org/10.3390/nano12071077.

[64] Hu X, Liu S, Zhou G, Huang Y, Xie Z, Jing X. Electrospinning of polymeric nanofibers for drug delivery applications. *J Control Release* **185**: 12–21 (2014). https://doi.org/10.1016/j.jconrel.2014.04.018.

[65] Zhao H, Chi H. Electrospun bead-on-string fibers: Useless or something of value? In: *Novel Aspects of Nanofibers*. London, UK: IntechOpen, 2018: 87–102. https://doi.org/10.5772/intechopen.74661.

[66] Albiladi A, Gzara L, Organji H, Alkayal N S, Figoli A. Electrospun poly(vinylidene fluoride-co-hexafluoropropylene) nanofiber membranes for brine treatment via membrane distillation. *Polymers* **15**(12): 2706 (2023). https://doi.org/10.3390/polym15122706.

[67] Zhou Z, Wu X-F. Electrospinning superhydrophobic–superoleophilic fibrous PVDF membranes for high-efficiency water–oil separation. *Mater Lett* **160**: 423–427 (2015). https://doi.org/10.1016/j.matlet.2015.08.003.

Just Accepted

[68] Bhairamadgi N S, Pujari S P, van Rijn C J M, Zuilhof H. Adhesion and friction properties of fluoropolymer brushes: on the tribological inertness of fluorine. *Langmuir* **30**(42): 12532–12540 (2014). https://doi.org/10.1021/la501802b.

[69] Dong Z-Q, Ma X-H, Xu Z-L, Gu Z-y. Superhydrophobic modification of PVDF-SiO_2 electrospun nanofiber membranes for vacuum membrane distillation. *RSC Adv* **5**(83): 67962–67970 (2015). https://doi.org/10.1039/C5RA10575G.

[70] Fukushima S, Karube Y, Kawakami H. Preparation of ultrafine uniform electrospun polyimide nanofiber. *Polym J* **42**(6): 514–518 (2010). https://doi.org/10.1038/pj.2010.33.

[71] He Y, Han D, Chen J, Ding Y, Jiang S, Hu C, Chen S, Hou H. Highly strong and highly tough electrospun polyimide/polyimide composite nanofibers from binary blend of polyamic acids. *RSC Adv* **4**(104): 59936–59942 (2014). https://doi.org/10.1039/C4RA10075A.

[72] Yao J, Pantano M F, Pugno N M, Bastiaansen C W M, Peijs T. High-performance electrospun co-polyimide nanofibers. *Polymer* **76**: 105–112 (2015). https://doi.org/10.1016/j.polymer.2015.08.053.

[73] Li J, Zhou N, Wong J S S. Tribological behavior of lubricant-impregnated porous polyimide. *Friction* **12**(4): 711–725 (2024). https://doi.org/10.1007/s40544-023-0796-9.

[74] Chen W, Wang W, Liang H, Zhu P. Study on lubricant release-recycle performance of porous polyimide retainer materials. *Langmuir* **38**(37): 11440–11450 (2022). https://doi.org/10.1021/acs.langmuir.2c01781.

[75] Tian L, Zhang C, He X, Guo Y, Qiao M, Gu J, Zhang Q. Novel reusable porous polyimide fibers for hot-oil adsorption. *J Hazard Mater* **340**: 67–76 (2017). https://doi.org/10.1016/j.jhazmat.2017.06.063.

[76] Topuz F, Abdulhamid M A, Nunes S P, Szekely G. Hierarchically porous electrospun nanofibrous mats produced from intrinsically microporous fluorinated polyimide for the removal of oils and non-polar solvents. *Environ Sci Nano* **7**(5): 1365–1372 (2020). https://doi.org/10.1039/D0EN00084A.

[77] Liu Y, Qian X, Wang L, Bai H, Cui Y. Electrospun polyimide nanofibrous membranes for absorption of oil spills. *J Ind Text* **50**(4): 584–595 (2020). https://doi.org/10.1177/1528083719838067.

[78] Mannarino M M, Katsumata R, Rutledge G C. Structural, mechanical, and tribological properties of electrospun poly(hexamethylene adipamide) fiber mats. *Wear* **305**(1): 58–68 (2013). https://doi.org/10.1016/j.wear.2013.05.010.

[79] Ren Y, Zhang L, Xie G, Li Z, Chen H, Gong H, Xu W, Guo D, Luo J. A review on tribology of polymer composite coatings. *Friction* **9**(3): 429–470 (2021). https://doi.org/10.1007/s40544-020-0446-4.

Just Accepted

[80] Mannarino M M, Rutledge G C. Mechanical and tribological properties of electrospun PA 6(3)T fiber mats. *Polymer* **53**(14): 3017–3025 (2012). https://doi.org/10.1016/j.polymer.2012.04.039.

[81] Dinc S K, Caglar B N, Birlik Demirel G, San Keskin N O. Preparation of non-toxic green slippery liquid infused surfaces based on electrospun fiber with anti-algae and anti-bacterial properties. *Polym Bull* **82**(9): 3463–3488 (2025). https://doi.org/10.1007/s00289-025-05679-6.

[82] Arashpour H, Jafari Nedoushan R, Akbarzadeh S, Fashandi H, Allafchian A, Lim H J. Epoxy/carbon fabric composite containing core-shell polystyrene electrospun fibers: integrated self-lubrication for enhanced wear resistance and mechanical performance. *Polym Compos* **47**(11): 9818–9827 (2026). https://doi.org/10.1002/pc.70862.

[83] Ahmed N, Nassar A. Lubrication and lubricants. In: *Tribology - Fundamentals and Advancements*. Gegner J, Ed. London, UK: IntechOpen, 2013: 55-76. https://doi.org/10.5772/56043.

[84] Manu B R, Gupta A, Jayatissa A H. Tribological properties of 2D Materials and composites—a review of recent advances. *Materials* **14**(7): 1630 (2021). https://doi.org/10.3390/ma14071630.

[85] Ye J, Burris D L, Xie T. A review of transfer films and their role in ultra-low-wear sliding of polymers. *Lubricants* **4**(1): 4 (2016). https://doi.org/10.3390/lubricants4010004.

[86] Jiang Z, Sun Y, Liu B, Yu L, Tong Y, Yan M, Yang Z, Hao Y, Shangguan L, Zhang S, Li W. Research progresses of nanomaterials as lubricant additives. *Friction* **12**(7): 1347–1391 (2024). https://doi.org/10.1007/s40544-023-0808-9.

[87] Rahman M M, Islam M, Roy R, Younis H, Al Nahyan M, Younes H. Carbon nanomaterial-based lubricants: review of recent developments. *Lubricants* **10**(11): 281 (2022). https://doi.org/10.3390/lubricants10110281.

[88] Klein J. Hydration lubrication. *Friction* **1**(1): 1–23 (2013). https://doi.org/10.1007/s40544-013-0001-7.

[89] Sorkin R, Kampf N, Zhu L, Klein J. Hydration lubrication and shear-induced self-healing of lipid bilayer boundary lubricants in phosphatidylcholine dispersions. *Soft Matter* **12**(10): 2773–2784 (2016). https://doi.org/10.1039/C5SM02475G.

[90] Martín-Alfonso M A, Rubio-Valle J F, Hinestroza J P, Martín-Alfonso J E, Franco J M. Environmentally friendly tailor-made oleodispersions of electrospun cellulose acetate propionate nanostructures in castor oil for lubricant applications. *Nano Mater Sci* **7**(1): 90–104 (2025). https://doi.org/10.1016/j.nanoms.2024.02.003.

[91] Borrego M, Martín-Alfonso J E, Sánchez M C, Valencia C, Franco J M. Electrospun lignin-PVP nanofibers and their ability for structuring oil. *Int J Biol Macromol* **180**: 212–221 (2021). https://doi.org/10.1016/j.ijbiomac.2021.03.069

Just Accepted

[92] Wang Y, Cheng L, Wen S, Zhou S, Wang Z, Deng L, Mao H-Q, Cui W, Zhang H. Ice-inspired superlubricated electrospun nanofibrous membrane for preventing tissue adhesion. *Nano Lett* **20**(9): 6420–6428 (2020). https://doi.org/10.1021/acs.nanolett.0c01990.

[93] Zheng J, Sen J, Meng Z, Dong G. Electrospun PVDF/CNT nanofiber membranes with synergistic optimization of tribological and piezoelectric properties for artificial joint implant coatings. *Mech Syst Signal Process* **240**: 113418 (2025). https://doi.org/10.1016/j.ymssp.2025.113418.

[94] Liu N, Liu M, Huang T, Yu B, Zhu M, Yu H. Synergistic interfacial crosslinking and solid lubrication enable durable all-fiber sliding triboelectric nanogenerators for wearable energy harvesting. *Chem Eng J* **546**: 179442 (2026). https://doi.org/10.1016/j.cej.2026.179442

[95] Ali A A, Eldesouky A R, Zoalfakar S H. Mechanical and tribological properties of hot-pressed electrospun MWCNTs/carbon nanofibril composite fabrics. *Int J Adv Manuf Technol* **74**(5): 983–993 (2014). https://doi.org/10.1007/s00170-014-6046-6.

Author biography



Myoung-Hwan Park currently serves as an associate professor of chemistry and life science and the director of the Research Center for the NanoBioMaterials Lab at Sahmyook University. His group is currently developing novel approaches and versatile materials for applications in drug delivery systems and industrial devices. He is also the founder and current CEO of NtoB Co. Ltd., specializing in drug delivery platforms for brain cancer and cosmetics, and NBChem Co. Ltd., which manufactures low-friction coating composites for mobile devices. Prior to his tenure at Sahmyook University, he completed his postdoctoral training in Paula Hammond's lab in the Department of Chemical Engineering at Massachusetts Institute of Technology (MIT). In 2012, he received his Ph.D. degree

Just Accepted

under the supervision of Prof. Vincent Rotello from the Department of Chemistry of the University of Massachusetts.



Yuri Park received her doctoral degree from Sahmyook University in 2023 and is currently affiliated with the NanoBioMaterials Lab at the Sahmyook University Convergence Science Center. She focused on researching and developing low friction materials and cosmetics in parallel through research on emulsion technology and nanobubbles.

Just Accepted